Title: Extensive transmission and variation in a functional receptor for praziquantel resistance in endemic *Schistosoma mansoni*

Authors: Duncan J. Berger[1]*, Sang-Kyu Park[2], Thomas Crellen[1,3], Tushabe John Vianney[4], Narcis B. Kabatereine[5], James A. Cotton[1,3], Richard Sanya[6] , Alison Elliot[6,7], Edridah M. Tukahebwa[5], Moses Adriko[5], Claire J. Standley[8], Anouk Gouvras[9], Safari Kinung'hi[10], Helmut Haas[11], Muriel Rabone[12], Aidan Emery[12], Poppy H. L. Lamberton[3], Bonnie L. Webster[12], Fiona Allan[12], Sarah Buddenborg[1], Matthew Berriman[1,13]*, Jonathan S. Marchant[2]*, Stephen R. Doyle[1]*, Joanne P. Webster[14]*

Affiliations:

1. Wellcome Sanger Institute, Wellcome Genome Campus, Hinxton, Cambridgeshire, CB10 1SA, UK
2. Department of Cell Biology, Neurobiology and Anatomy, Medical College of Wisconsin, Milwaukee, Wisconsin 53226, USA
3. School of Biodiversity, One Health, and Veterinary Medicine, University of Glasgow, Glasgow, UK
4. Division of Biomedical Engineering, University of Glasgow, G12 8LT Glasgow, UK.
5. Vector Borne & Neglected Tropical Disease Control Division, Ministry of Health, Kampala, Uganda
6. Immunomodulation and Vaccines Programme, Medical Research Council/Uganda Virus Research Institute and London School of Hygiene and Tropical Medicine Uganda Research Unit, Entebbe, Uganda.
7. Department of Infection Biology, London School of Hygiene and Tropical Medicine, London, UK
8. Center for Global Health Science and Security, Georgetown University, 3900 Reservoir Rd NW, Washington DC 20007, USA
9. Global Schistosomiasis Alliance, Podium Space - Ealing Cross, 85 Uxbridge Road, London, W5 5BW, UK

10. National Institute for Medical Research (NIMR) Mwanza Centre, P.O Box 1462, Mwanza, United Republic of Tanzania
11. helminGuard, Süelfeld, Germany
12. Department of Life Sciences, The Natural History Museum, London, SW7 5BD, UK
Wolfson Wellcome Biomedical Laboratories, Department of Life Sciences, The Natural History Museum, London, SW7 5BD, UK, London Centre for Neglected Tropical Disease Research (LCNTDR), London, UK
13. Current address: School of Institute of Infection & Immunity, College of Medical, Veterinary & Life Sciences, University of Glasgow, 120 University Place, Glasgow, G12 8TA, UK
14. Department of Pathology and Pathogen Biology, Royal Veterinary College, University of London, Herts, UK

* Corresponding authors
Underline - co-supervised this work

One Sentence Summary: Population genomics and functional genetics of praziquantel resistance in *Schistosoma mansoni*

Abstract: Mass-drug administration (MDA) of human populations using praziquantel monotherapy has become the primary strategy for controlling and potentially eliminating the major neglected tropical disease schistosomiasis. To understand how long-term MDA impacts schistosome populations, we analysed whole-genome sequence data of 570 *Schistosoma mansoni* samples (and the closely related outgroup species, *S. rodhaini)* from eight countries incorporating both publicly-available sequence data and new parasite material. This revealed broad-scale genetic structure across countries but with extensive transmission over hundreds of kilometres. We characterised variation across the transient receptor potential melastatin ion channel, $TRPM_{PZQ}$, a target of praziquantel, which has recently been found to influence praziquantel susceptibility. Functional profiling of $TRPM_{PZQ}$ variants found in endemic populations identified four mutations that reduced channel sensitivity to praziquantel, indicating standing variation for resistance. Analysis of

parasite infrapopulations sampled from individuals pre- and post-treatment identified instances of treatment failure, further indicative of potential praziquantel resistance. As schistosomiasis is targeted for elimination as a public health problem by 2030 in all currently endemic countries, and even interruption of transmission in selected African regions, we provide an in-depth genomic characterisation of endemic populations and an approach to identify emerging praziquantel resistance alleles.

INTRODUCTION

Schistosomiasis is a neglected tropical disease which currently infects 250 million people across 78 endemic nations (*1*, *2*). Infections are prevalent among children, including pre-school-aged children, as well as adults in low and middle-income countries, with 90% of infections occurring in sub-Saharan Africa. The etiological agents of schistosomiasis are freshwater snail-borne parasitic trematodes of the genus *Schistosoma* (principally *Schistosoma mansoni, S. japonicum,* and *S. haematobium*). These parasitic worms dwell in the host's blood vessels, often for years, where they lay eggs, many of which become trapped in host tissues, resulting in a spectrum of pathologies including anaemia, stunted growth, genital lesions, fever and irreversible organ damage (*3*). Recognising the severe and widespread impact of this disease, the World Health Organization (WHO) endorsed praziquantel monotherapy, distributed as part of mass drug administration (MDA) programmes, as the primary strategy for schistosomiasis control (*4*, *5*). In 2020 alone, 76.9 million people (representing 44.9% of those requiring treatment), predominantly school-aged children, were treated with praziquantel for schistosomiasis (*6*). Such treatment campaigns have resulted in an overall decrease in the prevalence of schistosomiasis among school-aged children by approximately 60% (*7*, *8*). Based on such successes, the WHO launched its 2021-2030 NTD roadmap and revised Guidelines for the Control and Elimination of Schistosomiasis (*1*). These set ambitious goals to eliminate schistosomiasis as a public health problem in all endemic countries (defined as reducing the proportion of heavy-intensity infections to <1%) and complete interruption of transmission in selected regions by 2030, primarily through the escalating use of praziquantel MDA (*9*).

99 Although MDA programmes have, in general, resulted in large-scale reductions in
100 schistosomiasis prevalence and morbidity in endemic regions (*7*, *10*, *11*), some of
101 these prevalence reductions have proven to be reversible over short timescales and,
102 despite years of repeated MDA, persistent hotspots of infection remain (*12*–*15*).
103 Ongoing surveillance projects have also revealed substantial heterogeneity in
104 infection prevalence, intensity and morbidity within and between endemic regions
105 (*16*–*18*). This includes potential variability in parasite response to praziquantel,
106 which, given the current lack of available vaccines or alternative antischistosomal
107 drugs, represents a major threat to the control and elimination of schistosomiasis
108 (*19*–*21*). In combination with other public health measures, MDA programmes are
109 expected to dramatically alter patterns of schistosome transmission and exert
110 selective pressure for praziquantel resistance. However, despite over twenty years of
111 MDA in some areas, there is no consistent evidence that sustained praziquantel
112 administration has impacted parasite population genetic structure or diversity (*22*–
113 *25*). Likewise, while there is clear evidence that resistance to praziquantel can be
114 rapidly selected for in laboratory settings (*26*–*29*), there is limited evidence of
115 established praziquantel resistance in endemic *S. mansoni* populations (*30*). This
116 contrasts with that of emerging or established heritable resistance, particularly in the
117 veterinary helminths, to every other class of anthelmintic used (*31*–*34*). Part of the
118 explanation lies in the fact that, until recently, we neither knew the precise mode of
119 action of praziquantel against schistosomes nor had any molecular markers to
120 monitor potential praziquantel resistance amongst natural *Schistosoma* spp.
121 populations. Recent efforts have, for the first time, identified the molecular target of
122 praziquantel, a transient receptor potential (TRP) melastatin ion channel
123 (*Sm*.TRPM$_{PZQ}$) (*35*–*38*). This discovery permits evaluation of praziquantel efficacy

124 and resistance risk, although such resistance-conferring alleles have only been
125 identified in a single isolate from endemic populations (*37*). Characterising the
126 transmission and recent evolution of schistosome populations is, therefore, of broad
127 epidemiological importance as a means to understand how parasite populations are
128 structured and how they are changing in response to interventions aimed at
129 controlling schistosomiasis.
130
131 Here, we have used whole-genome sequencing to characterise genomic variation
132 from globally dispersed populations of the major human infective species *S. mansoni*
133 (and the closely related outgroup species, *S. rodhaini)* (*39–41*). Our analyses focus
134 on populations within endemic regions of East Africa, primarily those found around
135 Lake Victoria, one of the largest foci of schistosomiasis infections and a target of
136 long-term MDA efforts (*7*, *20*). We aimed to quantify variation within the newly
137 identified candidate praziquantel resistance locus, *Sm*.TRPM$_{PZQ}$ (*36*, *37*, *42*), to
138 determine the prevalence of potential resistance-conferring mutations. This also
139 included extensive WGS of *S. mansoni* from within individual hosts before and after
140 praziquantel administration to quantify the immediate genetic impact of treatment.
141 These data raise significant implications regarding the standing variation of potential
142 praziquantel resistance in human schistosome population and represent an
143 important resource for assessing the efficacy of current interventions and guiding
144 future treatment strategies.
145

146 **RESULTS**

147 **The genetic diversity of geographically dispersed isolates supports high**
148 **transmission in endemic regions**

149 We analysed whole-genome sequence data from 574 *Schistosoma* samples (*n* =
150 570 *S. mansoni* and *n* = 4 *S. rodhaini* ; hereafter all referred to as accessions)
151 isolated from eight countries, including 207 new *Schistosoma* samples sequenced
152 for this study (Fig. 1A; Table 1; Supplementary Data 1) (*39–41*). Most accessions
153 were derived from Lake Victoria (88.3%), a major focus of *S. mansoni* infection.
154 These included published sequence data from miracidial samples isolated from
155 infected children between 2014 and 2017 from either the Koome & Damba Islands
156 (hereafter referred to as the Koome Islands; *n* = 174) (*41*) or Southern Uganda (*n* =
157 164) (*39*), with a median of two isolates sequenced per child (range 1-11). We
158 sequenced an additional 164 miracidia from just three children from Southern
159 Uganda (*n* = 89, 51 & 23 miracidia per child), including both pre- (*n* = 82) and post-
160 praziquantel treatment (*n* = 82) sampling (*20*). The only other Lake Victoria
161 accessions were derived from cercariae shed from snails captured in Northern
162 Tanzania (*n* = 31) or Southern Uganda (*n* = 2). Of the remaining samples, two were
163 cercariae from the shoreline of Lake Albert, four were cercariae from a passaged
164 strain originally isolated in Lake Albert, 17 were miracidia collected from children
165 living in Eastern Uganda, and ten were published adult-stage isolates of passaged
166 laboratory strains originally sampled from Kenya (*n* = 1), Senegal (*n* = 3), Cameroon
167 (*n* = 1), Guadeloupe (*n* = 4) or Puerto Rico (*n* = 1) (*40*). As an outgroup, we included
168 four *S. rodhaini* accessions, two cercarial isolates from Tanzania and two adult-stage
169 isolates of passaged lab strains from isolates originally sampled in Burundi. We
170 mapped sequence reads from all 574 accessions to the *S. mansoni* reference

171 genome, and after variant calling and quality control, we identified 35,146,249 single-
172 nucleotide polymorphisms (SNPs) and 6,632,156 indels across all accessions
173 (Supplementary Data 2).
174
175 To characterise population structure, we produced a maximum likelihood phylogeny
176 and performed principal component analysis using unlinked autosomal variants.
177 These analyses distinguished accessions sampled in East Africa from those in West
178 Africa and the Caribbean (Fig. 1B,C). The only exception was a single laboratory-
179 passaged isolate from coastal Kenya that clustered with West African accessions,
180 consistent with previous analyses of this sample (*40*, *43*). Within Eastern Africa,
181 populations from Lake Victoria, Lake Albert and Eastern Uganda formed distinct but
182 partially overlapping clusters. Pairwise measures of the fixation index (F_{ST}) showed
183 limited population differentiation between Lake Victoria, Lake Albert and Eastern
184 Uganda (range $F_{ST} = 2.49\times10^{-2} - 4.59\times10^{-2}$) and negligible differentiation between
185 Lake Victoria populations, despite the geographic separation of up to 300 km (range
186 $F_{ST} = 2.41\times10^{-3} - 4.07\times10^{-3}$, Supplementary Fig. 1A). East African populations had
187 comparable levels of nucleotide diversity (range median $\pi = 2.35\times10^{-3} - 3.35\times10^{-3}$;
188 Supplementary Fig. 1B) and effective population size (N_e) estimates (range N_e =
189 58,004-64,063; Supplementary Fig. 2; Supplementary Data 3) suggesting shared
190 recent population histories. Analyses of population ancestry for individual accessions
191 identified similar population compositions across all Lake Victoria populations with
192 variable ancestry contributions from Lake Albert and West African populations (Fig.
193 1F, Supplementary Data 4). Accessions from Eastern Uganda displayed variable,
194 mixed ancestry from Lake Victoria, Lake Albert and West Africa populations,
195 suggesting migration from multiple regions.

Ancestry analyses revealed low levels of *S. rodhaini* admixture (range: 0.00-2.32%), potentially indicative of interspecific hybridisation, across most unrelated *S. mansoni* accessions (Fig. 1D; Supplementary Data 4). In East Africa, *S. mansoni* and *S. rodhaini* are broadly sympatric and share both intermediate and definitive hosts, with *S. mansoni* infecting both specific primate and rodent species and *S. rodhaini* infecting rodents, allowing opportunities for inter-species pairings and hybridisation. However, due to the small number of *S. rodhaini* isolates included in this study (n = 4) and the lack of a non-admixed, outgroup population, the incidence of recent admixture and/or historic introgression was not investigated further.

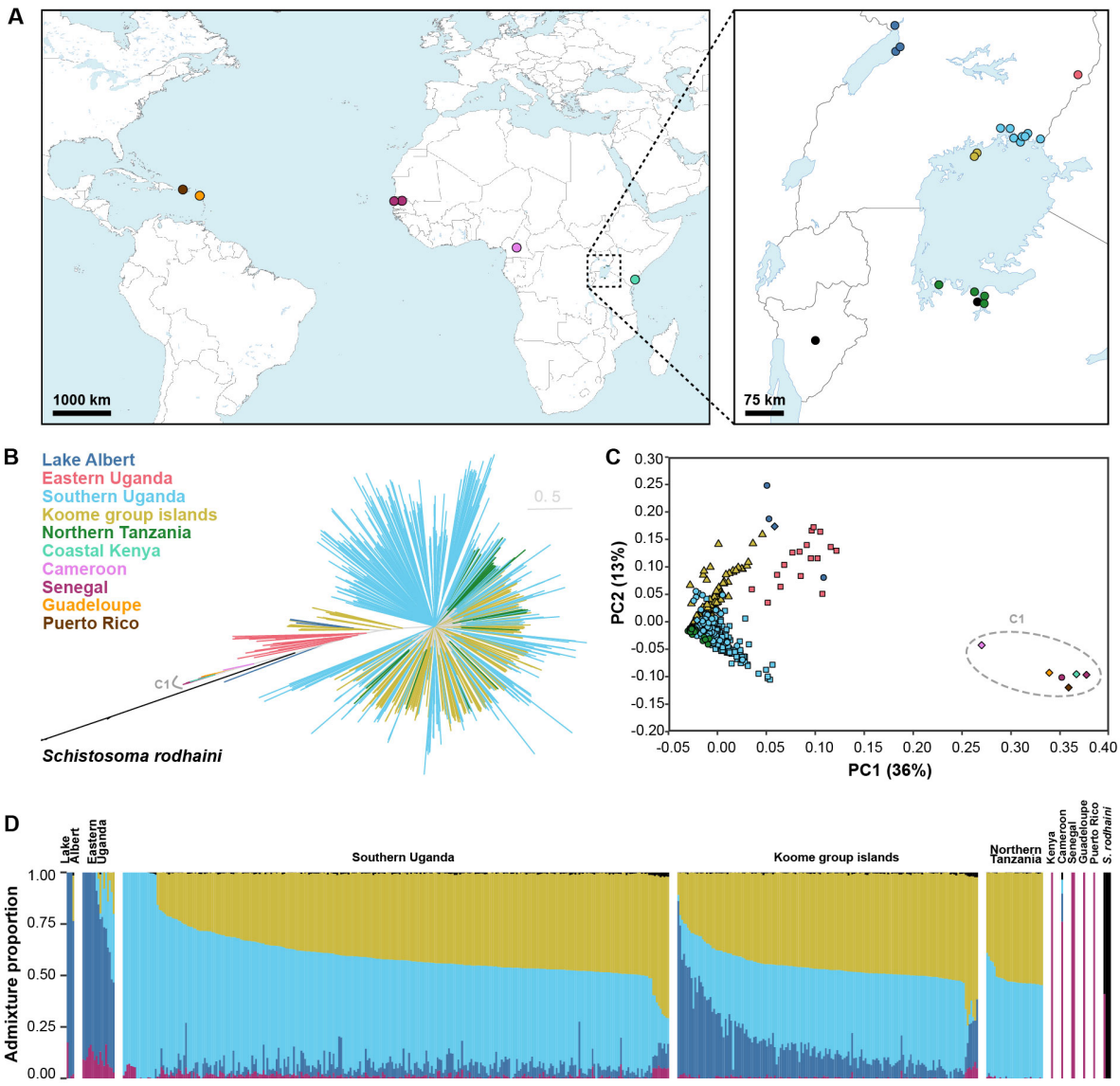

Fig. 1: Population structure of *Schistosoma* accessions. A. Global distribution of the 574 *Schistosoma* accessions used in this study. Sampling locations are coloured by geographical divisions: Puerto Rico (PR; brown), Guadeloupe (GP; orange), Senegal (SN; dark purple), Cameroon (pink), Coastal Kenya (KE; teal), Lake Albert (dark blue), Eastern Uganda (red), Southern Uganda (light blue), Koome group islands (yellow), Northern Tanzania (dark green). Black points represent the sampling coordinates of *S. rodhaini* accessions. **B.** The maximum-likelihood phylogenetic tree was inferred using 188,923 autosomal single-nucleotide polymorphisms (SNPs) and all 574 accessions. Branches are coloured based on the subdivisions described in a), and the tree is rooted on *S. rodhaini*.

Highlighted clade ‘C1’ represents all West African (Senegalese and Cameroonian), Caribbean (Puerto Rican and Guadeloupean) and Coastal Kenyan accessions. **C.** Principal component analysis (PCA) of genetic differentiation between 505 unrelated *S. mansoni* accessions using 214,445 autosomal SNPs. Points are coloured and shaped based on the groups described in (A). **D.** ADMIXTURE plots illustrating the inferred ancestry of 505 unrelated *S. mansoni* and four *S. rodhaini* accessions. Here, we assume five populations (K) are present, inferred using 10-fold cross-validation and a standard error estimation with 250 bootstraps. Y-axis values show the admixture proportions for each accession, and colours for each population were assigned based on the majority ancestry of each geographical division.

234 **Table 1: Sample information and history of praziquantel treatment.**

Species	Country	Region	Development Stage			Sampling stage			Reference
			Adults	Cercariae	Miracidia	Pre-treatment	Post-treatment	Not applicable	
S. mansoni	Uganda	Lake Albert	1	6	0	0	0	7	Herein; Crellen et al. 2016
	Uganda	Eastern Uganda	0	0	17	17	0	0	Berger et al. 2021
	Uganda	Southern Uganda	1	2	328	201	127	3	Herein; Berger et al. 2021
	Uganda	Koome Islands	0	0	174	123	51	0	Vianney et al. 2022
	Tanzania	Northern Tanzania	0	31	0	0	0	31	Herein
	Kenya	Coastal Kenya	1	0	0	0	0	1	Crellen et al. 2016
	Cameroon		1	0	0	0	0	1	Crellen et al. 2016
	Senegal		3	0	0	0	0	3	Herein; Crellen et al. 2016
	Puerto Rico		1	0	0	0	0	1	Crellen et al. 2016
	Guadeloupe		4	0	0	0	0	4	Crellen et al. 2016
S. rodhaini	Tanzania	Northern Tanzania	0	2	0	0	0	2	Herein
	Burundi		2	0	0	0	0	2	Herein; Crellen et al. 2016

235

236 This study included 574 accessions, sequenced from parasite samples derived from snail hosts (cercariae), humans (miracidia) or laboratory-
237 passaged strains (adults). Publicly-available data (*n* = 339) and new sequencing data (*n* = 208; defined as “herein”) were generated for this
238 study. Miracidia accessions were sampled pre-treatment with praziquantel (40 mg/kg) or four weeks post-treatment.

239 **Functionally relevant genomic variation influences praziquantel sensitivity**

240 A transient receptor potential (TRP) melastatin ion channel (*Sm.*TRPM$_{PZQ}$;
241 *Smp_246790*) has recently been proposed as the target of praziquantel (*35*–*38*).
242 This candidate gene underlies variation in praziquantel susceptibility, at least within
243 schistosome laboratory populations (*35*–*37*, *44*). Mutagenesis of key residues within
244 the praziquantel binding site of TRPM$_{PZQ}$ (located in the transmembrane voltage-
245 sensor-like domain, VSLD) resulted in the loss of sensitivity to praziquantel (*36*).
246

247 Consistent with previous genomic surveys (*39*, *41*), analysis of haplotype diversity
248 using the integrated haplotype score (iHS) did not suggest that *Sm.*TRPM$_{PZQ}$ was
249 under positive selection in Lake Victoria populations (Supplementary Fig. 3,
250 Supplementary Data 5,6). However, analysis of variation within *Sm.*TRPM$_{PZQ}$
251 identified a high degree of variability with a predicted 496 amino acid changes at
252 433/2268 residues (Fig. 2), with mutations at 174 of these residues found only in
253 single accessions (Supplementary Data 7). We generated point mutations to modify
254 12 *Sm*.TRPM$_{PZQ}$ residues, and used an *in vitro* Ca^{2+} reporter assay (*35*) to assess
255 their impact on *Sm*.TRPM$_{PZQ}$ function. Eight of these mutants, all conservative amino
256 acid substitutions, exhibited similar praziquantel sensitivity (range EC_{50} = 0.49-0.96
257 μM) to the wild-type *Sm*.TRPM$_{PZQ}$ channel (EC_{50} = 0.74 μM [standard error (SE) =
258 0.17]; Fig. 3A; Supplementary Data 8; Supplementary Fig. 4). Mutants p.T1624K and
259 p.R1843Q exhibited a decreased sensitivity to praziquantel (EC_{50} = 1.41 μM [SE =
260 0.23] and EC_{50} = 1.11 μM [SE = 0.08], respectively) and two mutants (p.Y1554C,
261 p.Q1670K) caused a complete loss in praziquantel sensitivity (Fig. 3B;
262 Supplementary Data 8; Supplementary Fig. 5).
263

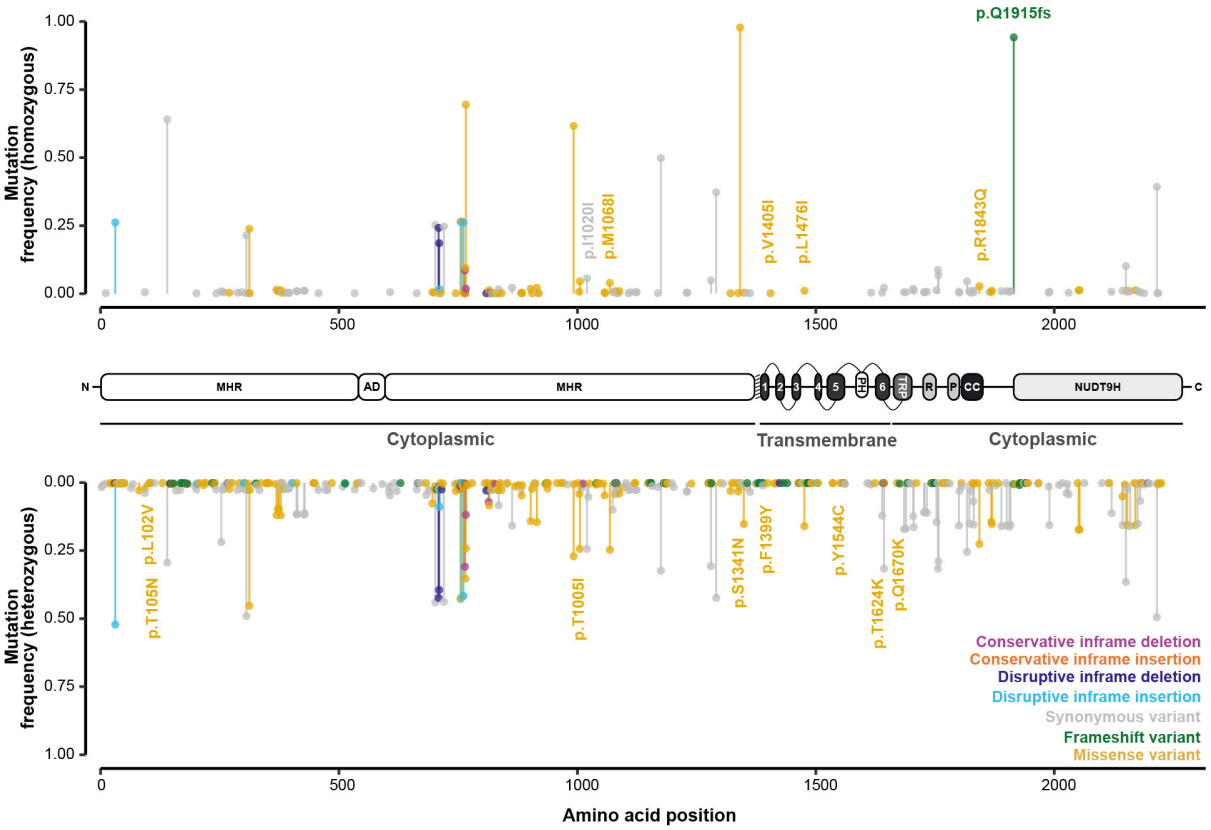

Fig. 2: Genetic variation in the candidate mediator of praziquantel susceptibility, the transient potential receptor channel *Sm.*TRPM$_{PZQ}$. Mutational frequency along the protein structure of *Sm.*TRPM$_{PZQ}$ (*Smp_246790*). Frequencies of mutations are reported across 550 *S. mansoni* accessions (y-axis), representing samples from Eastern Uganda (*n* = 17), Southern Uganda (*n* = 328), the Koome islands (*n* = 174) and Northern Tanzania (*n* = 31). X-axis values represent the location of the mutations on the protein, and bars (and terminal points) are coloured by the predicted impact of each mutation. Structure of *Sm.*TRPM$_{PZQ}$: N-terminal TRPM homology region (MHR) domain, ankyrin-like repeat domain (AD), pre-S1 helix (shaded), TM-spanning helices (1-6), pore helices (PH), TRP domain (TRP), rib helices (R), pole helices (P), coiled-coil (CC) region and the COOH terminal NUDT9H domain (NUDT9H).

279 Seven of the twelve mutations mapped within an existing homology model for the
280 transmembrane-spanning region of *Sm*.TRPM$_{PZQ}$, enabling structural insight into
281 these functional effects (Fig. 3C) (*36*). Four mutations had no impact on praziquantel
282 action (p.V1405I, p.L1476I, p.S1341N & p.F1399Y; Fig. 3A): p.V1405I and p.L1476I
283 are found within extracellular loops of the channel, p.S1341N lies the COOH-terminal
284 cytoplasmic domain and p.F1399Y, while within the voltage-sensor like domain
285 (VSLD) of the channel that harbours the praziquantel binding site, is remote (~10Å
286 away) from the praziquantel binding poise (Fig. 3C). Mutation p.T1624K (~2-fold
287 lower sensitivity; Fig. 3B) projects into the extracellular milieu before the start of S6
288 and may cause sub-optimal orientation of the S6 helix. The other variant associated
289 with lower sensitivity (p.R1843Q; Fig. 3B) lies outside the existing TRPM$_{PZQ}$
290 homology model but is predicted to localise within the COOH-terminal coiled-coil
291 region of the channel, which is involved in subunit interaction (*45*). Tetramer
292 misfolding and lower channel expression would explain the decreased sensitivity of
293 this variant.
294
295 The first of the two mutations that caused a complete loss of praziquantel sensitivity
296 (Fig. 3B), p.Y1554C, is found in the S5 helix (Fig. 3C). This residue projects toward
297 S6, where it is predicted to interact with a tyrosine residue (Y1636) in the S6 helix.
298 This cysteine mutant would be expected to disrupt this interaction, which is likely
299 important for the appropriate orientation of the helices that form the pore-forming
300 domain. The second, p.Q1670K, introduces a positive charge within the intracellular
301 TRP helix close to the bilayer interface. This is a critical region for channel gating,
302 and the mutation likely impacts the orientation of the TRP helix relative to the bilayer
303 and interactivity with the S4/S5 loop of *Sm*.TRPM$_{PZQ}$, which regulates TRPM channel

activation (*46*). The deleterious effects of p.Y1554C and p.Q1670K are, therefore, consistent with the known importance of these regions for channel function (*36*).

Of the four mutations that decreased or eliminated praziquantel sensitivity, three (p.Y1554C, p.Q1670K, p.T1624K) were only found in a heterozygous state in single accessions (Supplementary Data 7,9,10). p.R1843Q was far more common, with homozygous variants (c.5528G>A) identified in 3.68% (*n* = 21 accessions across the entire dataset; *n* = 15 miracidia from 12 individuals) of accessions and heterozygous in 22.6% of accessions (*n* = 129 accessions across the entire dataset; *n* = 120 miracidia from 68 individuals). This variant was also more prevalent in post-treatment populations (5.05% of post-treatment accessions; *n* = 9 miracidia from 8 individuals) compared to pre-treatment populations (1.75% of pre-treatment accessions; *n* = 6 miracidia from 4 individuals; Supplementary Data 10), although accessions with this variant (and all other evaluated variants) did not form a distinct subpopulation (Supplementary Fig.s 6-9). In addition to the mutations analysed via targeted mutagenesis, we identified a second high-prevalence homozygous frameshift mutation, p.Q1915fs, in 94.0% of accessions. Park and colleagues (*36*) reported that truncation mutations (Δ1914) of the C-terminal NUDT9H domain do not impact the TRP channels' responsiveness to praziquantel.

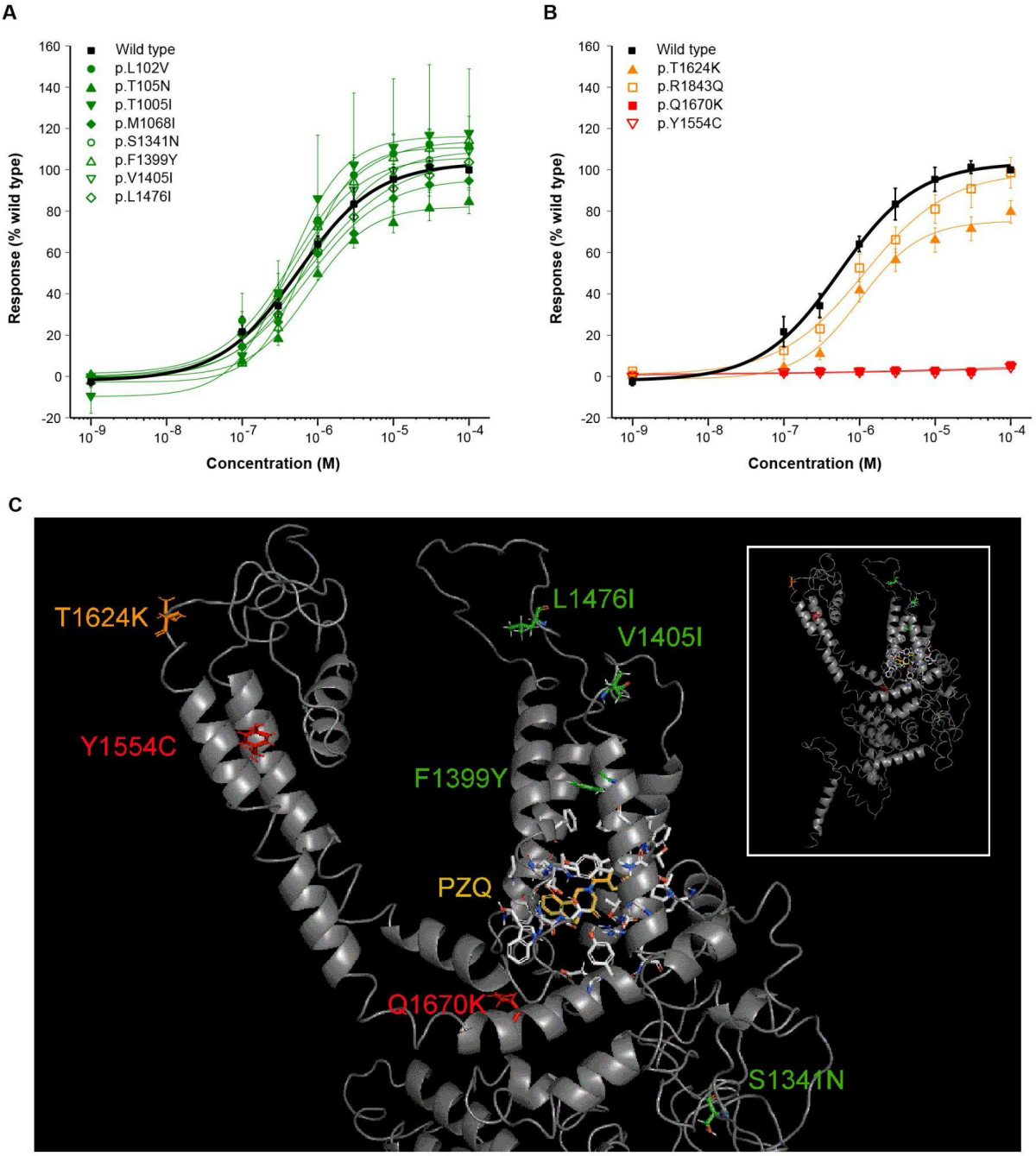

Fig. 3: Functional profiling of variants of the transient potential receptor channel *Sm*.TRPM$_{PZQ}$. Concentration-response relationships for consensus Sm.TRPM$_{PZQ}$ sequence compared with twelve Sm.TRPM$_{PZQ}$ variants, which exhibit an average EC_{50} to ±PZQ of **(A)** <1 µM (green) or **(B)** >1 µM (orange). Constructs for which no praziquantel-evoked activity was observed (Y1554C, Q1670K) are shown in (b) in red. Results represent mean±sem from at least three independent transfections. **C.** *Inset*, homology model of the transmembrane spanning region (residues 1100 to 1800) of a *Sm*.TRPM$_{PZQ}$ monomer from

333 [2]. The enlarged view shows the location of the functionally profiled variants. Praziquantel
334 and residues within 5Å of the praziquantel binding poise (white) are shown at the base of the
335 voltage-sensor-like domain (VSLD) of the channel, with the S5 and S6 pore-forming helices
336 to the left.
337
338
339
340 Le Clec'h and colleagues recently identified three putative marker variants for
341 praziquantel resistance in selected laboratory lines (*37*). The first of these was a
342 homozygous SNP predicted to result in a synonymous mutation (*Sm.*TRPM$_{PZQ}$-
343 2723187C; p.I1020I), which we identified in 6.14% (*n* = 35, *n* = 30 miracidia from 21
344 individuals) of accessions (Supplementary Data 7,9,10). This mutation was nearly
345 twice as common in post-treatment populations (8.43% of accessions; *n* = 15
346 miracidia from 10 individuals) compared to pre-treatment populations (4.40% of
347 accessions; *n* = 15 miracidia from 13 individuals). A further 24.9% of accessions had
348 a single copy of this marker. The second and third markers were 150 kb deletions
349 adjacent to *Smp_246790* (~1.22 Mb) and *Smp_345310* (~3.18-3.33 Mb),
350 respectively. Structural variant genotyping did not identify the former variant in our
351 accessions, but we did find a series of long homozygous deletions (69.9-215.0 kb)
352 located between 3.02-3.36 Mb in 43.3% of genotyped accessions (*n* = 170 of 393
353 genotyped accessions; Supplementary Data 11, Supplementary Fig. 10). However,
354 the 150 kb deletion was not enriched in post-treatment populations, and neither the
355 deletion nor p.I1020I clustered phylogenetically (Supplementary Fig. 9).
356
357

358 **Host infrapopulations reveal the extent of genetic relationships and evidence**
359 **of treatment failure**
360 Sampling and analysis of the parasite population from within a single host (defined
361 as the 'infrapopulation') across specific time points has the potential to identify
362 instances of treatment failure, which may be indicative of praziquantel resistance.
363 However, these infrapopulations are thought to be highly heterogeneous (*25*, *47*,
364 *48*), and previous genomic surveys of *S. mansoni* have only included small numbers
365 of parasites from the same individuals (max n = 11) (*39*, *41*, *49*, *50*) reducing the
366 likelihood of identifying related parasites. To provide greater resolution of
367 infrapopulation structure and evaluate the impact of praziquantel treatment, we
368 analysed pairwise kinship between 164 sequenced miracidia sampled pre- or post-
369 praziquantel treatment from a total of three donors: Bb1 (n = 47 pre-treatment, n =
370 42 post-treatment), Bu3 (n = 33 pre-treatment, n = 19 post-treatment) and Bu1 (n = 2
371 pre-treatment, n = 21 post-treatment) and reanalysed the 174 accessions from the
372 Vianney et al. (*41*) survey (98 donors, n = 123 pre-treatment, n = 51 post-treatment).
373

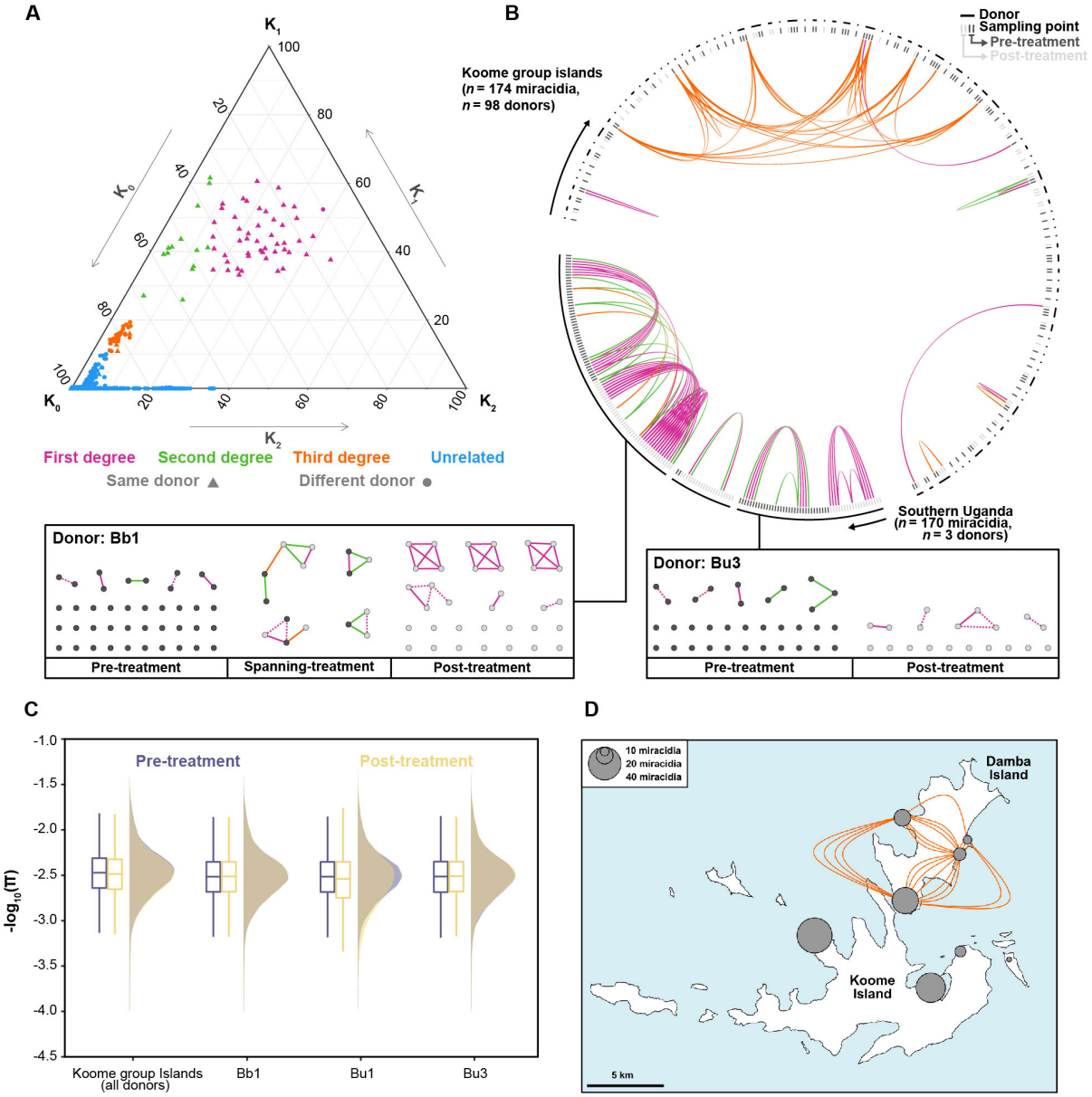

Fig. 4: Relatedness between *Schistosoma mansoni* accessions from endemic regions. **A.** Ternary plots representing pairwise relationships between accessions using the three relatedness coefficients K_0, K_1, and K_2, representing the probabilities that at a given locus, the two accessions shared zero, one or two-allele identity-by-descent, respectively. Each point represents a pairwise relationship between two accessions, showing whether each accession was from the same (triangles) or different (circles) donor. Points are coloured by the inferred relationship: first-degree (pink), second-degree (green), third-degree (orange) or unrelated (blue). Only accessions from three Southern Ugandan donors and all Koome

384 Island donors are shown. **B.** Inferred relationships within and between donors. The outer
385 lines represent each donor; within each line, individual accessions are shown coloured by
386 whether they were sampled before (dark grey) or after (light grey) treatment with
387 praziquantel. Coloured lines represent the same pairwise relationships as a). For donors
388 Bb1 and Bu3, all relationships are shown below the circular plot and shown in boxes where
389 they are grouped into pre-treatment samples, post-treatment samples, and pre- and post-
390 treatment samples (spanning treatment). Within the boxes, dotted lines represent
391 relationships inferred by NgsRelate but were found to have a lower degree or no-relation by
392 Sequoia. **C.** The effect of praziquantel treatment on nucleotide diversity (π) was calculated
393 for each donor infrapopulation (Bb1, Bu1 and Bu3) and all Koome group island samples.
394 Nucleotide diversity was calculated in 5 kb non-overlapping windows across each autosome
395 for each pre-treatment (purple) and post-treatment (yellow) population (including related
396 samples). For all boxplots, the central line indicates the median, and the top and bottom
397 edges of the box indicate the 25th and 75th percentiles, respectively. The maximum whisker
398 lengths are specified as 1.5 times the interquartile range. **D.** Identification of a circulating
399 lineage of *S. mansoni* on Damba Island (the northernmost island of the Koome group
400 islands). We identified a cluster of nine accessions, all with third-degree identical by descent
401 relationships, which clustered phylogenetically with accessions from Lake Albert.
402
403
404 We identified 49 first-degree relationships, 13 second-degree relationships and 34
405 third-degree relationships (Fig. 4A; Supplementary Data 12). Forty-seven of the 49
406 first-degree relationships were between accessions sampled from the same donor;
407 the remaining two were between donors and have previously been identified as
408 potentially mislabelled accessions (*41*). Estimates of the coefficient of inbreeding (*f*)
409 using the condensed identity coefficients also revealed low levels of inbred
410 relatedness (median $f = 0.000227$; range $f = 1\times10^{-6}$ - 0.35) in 18.8% of parents

411 (Supplementary Data 13) (*51*). Within infrapopulations of donors Bb1, Bu1 and Bu3,
412 we identified three first-degree relationships between pre-treatment accessions and
413 23 between post-treatment accessions. Most of these were found in infrapopulations
414 from Bb1, represented by three independent clusters of four accessions (Fig. 4B,C).
415 We also identified one first-degree and four second-degree relationships spanning
416 treatment arms, suggesting bi- and uni-parental survival, respectively. Both of the
417 first-degree relatives were also homozygous for the *Sm.*TRPM$_{PZQ}$-2723187C marker;
418 however, none of the second-degree relatives had a homozygous or heterozygous
419 copy. Additionally, we did not identify any homo- or heterozygous variants of
420 p.R1843Q in any of the first- or second-degree relatives spanning treatment. We
421 also found no evidence of reduced nucleotide diversity in post-treatment populations
422 (Fig. 4C) and low genetic differentiation between pre- and post-treatment populations
423 (range mean F_{ST} = 1.24×10^{-3} - 1.75×10^{-3}, Supplementary Fig. 11).
424
425 Examination of third-degree relationships within the Vianney and colleagues (*41*)
426 dataset identified a cluster of nine related accessions, all localised to Damba Island
427 and found in all four of the sampled villages (Fig. 4B,D). Phylogenetic analysis
428 showed all nine formed a distinct clade with six accessions from Lake Albert
429 (Supplementary Fig. 12), suggesting that these are derived from a recently imported
430 lineage from Lake Albert, recently dispersed across Damba Island.
431

432 **DISCUSSION**

433 As efforts to interrupt transmission and eliminate schistosomiasis as a public health
434 problem intensify over the next decade, the escalating use of MDA is expected to
435 result in increased selective pressures, altered transmission dynamics and
436 widespread reductions in schistosome populations (*1*, *9*). The consequences of such
437 large-scale changes to schistosome populations are unclear but provide a strong
438 incentive for genomic surveillance to detect and monitor such changes. In this study,
439 we have, to our knowledge, assembled the most comprehensive collection of
440 *Schistosoma* whole-genome sequencing data to date*,* including samples from across
441 eight countries and two major foci of infection.

442

443 Praziquantel resistance represents a credible threat to schistosomiasis control if it
444 were to establish in endemic populations. Despite over 50 years of use, $TRPM_{PZQ}$
445 has only recently been identified as a direct target of praziquantel and a genetic
446 determinant of reduced praziquantel susceptibility (*36*, *37*). We identified extensive,
447 low-frequency variation within this gene and used this variation database to inform
448 the targeted mutagenesis of 12 residues, focusing on mutations at potential key
449 residues. We identified four mutations in our population genetic analyses that
450 reduced or ablated channel responsiveness to praziquantel functional genetic *in vitro*
451 assays, and while only one (p.R1843Q) was present in more than a single
452 accession, all represent standing variation for praziquantel resistance in endemic
453 populations. Both p.R1843Q and p.I1020I (the latter a marker for praziquantel
454 resistance in passaged laboratory lines (*37*)) variants were present in multiple
455 accessions, indicating potential variability in praziquantel efficacy in these
456 populations. Both mutations were also more prevalent in post-treatment parasite

457 populations than their pre-treatment counterparts. However, our analyses and others
458 (*23*, *25*, *39*) have shown that post-treatment populations do not typically represent
459 subpopulations of pre-treatment parasites, which may result from reinfection or
460 under-sampling. It is possible that the increased prevalence of these mutations is
461 unrelated to praziquantel administration. It is clear, nevertheless, that despite the
462 asymmetrical per-host sampling of this study, these variants remain widespread in
463 parasite populations sampled from a wide range of hosts, showing that they are
464 prevalent across Lake Victoria. Further work should also be undertaken to determine
465 to what extent the mutations we identified impact the *in vivo* efficacy of praziquantel
466 and parasite fitness. Profiling these specific SNPs in the context of other changes
467 within $TRPM_{PZQ}$ in the same samples, reflecting broader allelic variation, is also
468 necessary.
469
470 Our analyses have demonstrated how genomic surveillance of parasites can help
471 identify variants contributing to reduced praziquantel efficacy in endemic populations
472 and provide structural and functional insights into $TRPM_{PZQ}$ that will permit a better
473 understanding of praziquantel efficacy in schistosomes. While we only characterised
474 a small proportion of the total variation we observed, our results survey genetic
475 variation within endemic regions where praziquantel has seen extensive use. These
476 data provide candidate variants for functional investigations and serve as a database
477 of variation for retrospective surveys once further resistance-conferring mutations
478 are identified. However, it is notable that a large proportion of our dataset was
479 derived from donors living in regions of long-term praziquantel administration.
480

481 Targeted mutagenesis identified four mutations in endemic populations that reduced
482 channel sensitivity to praziquantel, indicating standing variation for resistance. Whilst
483 we did identify both standing variation for future resistance evolution and instances
484 of treatment failures here, the apparent lack of obvious high-frequency resistance-
485 conferring mutations is encouraging as these populations have been under long-term
486 MDA pressure. The variable coverage of MDA may have allowed substantial refugia
487 populations to exist in untreated humans, snails and animal reservoirs. Refugia
488 would reduce the selection pressure for resistance, an approach that has been
489 deliberately employed in veterinary systems (*52*–*54*). Alternatively, reduced
490 praziquantel susceptibility might be linked to regulatory changes in expression or
491 RNA splicing (*37*), neither of which would be identified by our analyses. Considering
492 how recently *Sm.*TRPM$_{PZQ}$ was recognised as a mediator of praziquantel sensitivity,
493 future functional investigations will likely reveal additional relevant variants.
494
495 Despite involving a small number of donors, our analyses of host infrapopulation
496 dynamics represent the most thorough genomic characterisation of a host
497 infrapopulation of any parasitic helminth. Our analyses found that host
498 infrapopulations are exceptionally diverse, consistent with both autopsy studies and
499 genetic surveys, which have found that individual worm burdens range from one up
500 to hundreds or thousands of worm pairs per individual in low and high-endemicity
501 regions, respectively (*55*, *56*). Despite this, we did find evidence of sibling
502 relationships within both treatment arms, with indications of a higher degree of post-
503 treatment relatedness. We also found evidence of post-treatment parental survival,
504 suggesting either ineffective treatment or higher praziquantel tolerance within these
505 populations. However, the limited number of these accessions limited any formal

analyses of the possible genetic basis of reduced praziquantel efficacy. Consistent with previous genetic studies, these only represented a small proportion of the overall post-treatment populations (*25*), suggesting that most post-treatment samples represent either infection with additional parasites and/or parasites missed in pre-treatment sampling.

To conclude, we have characterised endemic *S. mansoni* populations at multiple spatial scales ranging from comparisons across major foci of infection to individual parasite infrapopulations. Our variation analysis within a candidate praziquantel resistance loci enabled us to identify multiple novel resistance-conferring mutations. These remain at low frequencies in studied populations but demonstrate standing variation from praziquantel resistance in endemic populations undergoing MDA. Our analyses also provide a resource for retrospective or confirmatory support of functional analyses of this recently identified locus. Finally, our extensive sequencing of host infrapopulations provided an in-depth genomic characterisation of parasite diversity and how this is impacted by praziquantel treatment. Overall, our study summarises *S. mansoni* genomic diversity and represents a resource to assess the efficacy of current interventions and guide future treatment strategies.

527 **MATERIALS AND METHODS**

528 The data analysed here incorporated whole-genome accessions from published
529 datasets from eight countries and 205 new *Schistosoma* sample data (Fig. 1A; Table
530 1; Supplementary Data 1). The sections below describe the origin, collection, and
531 ethical approval of samples, focusing only on the parasite samples sequenced for
532 this study and not previously published accessions.

533

534 **Collection and ethical approval for the sampling of Ugandan miracidia**

535 The collection of all Ugandan miracidial samples was undertaken as part of the
536 monitoring, evaluation and disease control activities conducted by the Vector Control
537 Division of the Ministry of Health (Uganda), the Schistosomiasis Control Initiative and
538 Imperial College London. All methods and data collection were approved by the
539 Uganda National Council for Science and Technology (Memorandum of
540 Understanding: sections 1.4, 1.5, 1.6) and the Imperial College Research Ethics
541 Committee (EC NO: 03.36. R&D No: 03/SB/033E). The Head of the Vector Control
542 Division informed local district officials, and the headteachers of each school were
543 informed about the study and requested to provide informed consent to allow
544 sampling to be performed within the school. Parents of the children were informed of
545 the study through school meetings, where they were provided with detailed
546 information regarding the purpose of the study and technical staff were present to
547 answer questions. Parents were requested to provide informed consent for their
548 children to participate in the study, and in addition, any children aged ten or older
549 were asked to give informed consent after receiving complete information about the
550 study. Participation was voluntary, access to treatment was not dependent on

551 participation in the study, and children could withdraw or be withdrawn from the
552 study at any time.
553
554 Stool samples were collected from each child, and duplicate Kato-Katz thick smears
555 were conducted (*57*). A Pitchford–Visser funnel was used to wash and filter parasite
556 eggs from the remaining stool sample, and the filtrate was stored overnight (*58*).
557 Miracidia were hatched the following day and were transferred into two sequential
558 dishes of nuclease-free water to dilute bacterial contaminants before being
559 individually fixed onto Whatman FTA-indicating classic cards (*59*, *60*). Between 1-3
560 days following testing, children with evidence of parasitic infection were treated with
561 praziquantel (40 mg/kg) for schistosomiasis and albendazole (400 mg) for soil-
562 transmitted helminths. Children were retested 25-27 days following treatment, and in
563 cases of incomplete *S. mansoni* clearance, miracidia were sampled again, and
564 treatment was re-administered.
565
566 **Collection and ethical approval for the sampling of Ugandan *S. mansoni***
567 **cercariae**
568 The FTA-preserved Ugandan *S. mansoni* cercariae were collected as part of snail
569 collection surveys conducted between 2007 and 2010 as part of the EU-CONTRAST
570 programme, a consortium of European and African researchers (CONTRAST
571 EU/INCO.Dev contract No. 032203) in association with the Schistosomiasis Control
572 Initiative (*61*) and provided via SCAN. The Ethical Review Board of the Uganda
573 National Council of Science & Technology approved the surveys.
574

575 **Collection and ethical approval for the sampling of Tanzanian *S. mansoni***
576 **cercariae**
577 Tanzanian *S. mansoni* cercariae were originally collected as part of snail collection
578 surveys undertaken in the Mwanza region and Geita regions of Northern Tanzania
579 between January 2012 and December 2015 (*62*) as part of the Schistosomiasis
580 Consortium for Operational Research and Evaluation (SCORE) snail project (*63*) and
581 archived within the Schistosomiasis Collection at the Natural History Museum
582 (SCAN) (Emery et al., 2007). Survey sites were picked based on their proximity
583 (within 5-15 metres) to schools and were identified based on local information about
584 water activities (bathing, fishing, water collection) (*63*). *Biomphalaria* spp. snails were
585 collected by scooping using handheld metal sieve scoops or dredging using a metal
586 dredge dropped from a boat and dragged 10 m back to shore. Scooped/dredged
587 snails were hand-collected with forceps and placed into collection jars. All snails
588 were placed in 24-well ELISA plates under direct light for at least four hours to
589 induce shedding, and cercariae from each shedding snail were individually collected
590 in 3 µL of water using a Gilson pipette and fixed on Whatman FTA cards (*59*, *60*).
591 COX-1 identification of *S. mansoni* was performed as described in Gouvras *et al.*
592 *(62)*.
593
594 **Origin of the Senegalese *S. mansoni* laboratory (adult worm) sample**
595 Both *S. mansoni* Senegalese isolates (FS0001 and FS0002) originated from
596 approximately 30 *Biomphalaria pfeifferi* with patent *S. mansoni* infections found in
597 the Western principal irrigation canal in the Ndiengue District of Richard Toll (*64*).
598 The strain was originally sampled in 1993 and then maintained at the School of

599 Biological Science, University of Wales (Bangor, United Kingdom) and subsequently
600 in the helminGuard laboratory (Süelfeld, Germany) (*65*).
601
602 **Origins of the *S. rodhaini* (adult worms and cercariae) samples**
603 The adult *S. rodhaini* adult worm sample (RZ0001) was provided by SCAN from a
604 laboratory-passaged *S. rodhaini* strain originally isolated from infected *Biomphalaria*
605 snails collected in Burundi in 2000. The sample used here represented the 6th
606 passage through laboratory *Biomphalaria glabrata* and *Mus musculus*, under the
607 Home Office project license numbers 70/4687 (before 2003) and 70/5935 (2003-
608 2008) (*59*).
609
610 The two *S. rodhaini* cercariae analysed here originated from the Mwanza region of
611 Tanzania. They were collected as part of the SCORE xenomonitoring project and
612 provided by SCAN. Species identification was confirmed by Sanger sequence
613 analysis of a partial region of the *cox1* gene, the ITS1+2 rDNA region, and a partial
614 region of the 18S rDNA region using the methods described in Pennance *et al*.,
615 2020.
616
617 **DNA extraction and sequencing**
618 The DNA from individual miracidia and cercariae were isolated from the Whatman
619 FTA cards using methods described by (*66*, *67*). A 2mm Harris micro-punch was
620 used to punch out the FTA disc containing the DNA. Within a well of a 96 PCR plate,
621 individual samples on individual punches were lysed in 30 µL of the following buffer:
622 30 mM Tris–HCl pH 8.0 (Sigma Aldrich), 0.5% Tween 20 (Sigma Aldrich), 0.5%
623 NP40/IGEPAL CA-630 (Sigma Aldrich) and 1.25 µg/mL of Protease reagent (Qiagen;

624 cat 19155). Punches were incubated at 50°C for 1 h, then heated to 75°C for 30
625 mins. DNA was extracted from adult worms using the Qiagen MagAttract HMW kit
626 (PN-67653) following the manufacturer's instructions. The DNA from the two
627 individual Senegalese adult worms was extracted using the Qiagen MagAttract HMW
628 kit (PN-67653) following the manufacturer's instructions.
629
630 Library preparation was performed using a low-input enzymatic fragmentation-based
631 library preparation method (*68*). For each sample, 20 µL of lysate (or extracted DNA)
632 was mixed with 50 µL of TE buffer (Ambion 10 mM Tris-HCL, 1 mM EDTA) and 50
633 µL of Ampure XP beads followed by a 5 min binding reaction at room temperature.
634 Magnetic bead separation was used to separate genomic DNA, which was then
635 washed twice with 75% ethanol. Beads were resuspended in 26 µL of TE buffer. To
636 perform DNA fragmentation and A-tailing, each sample was immediately mixed with
637 7 µL of 5x Ultra II FS buffer and 2 µL of Ultra II FS enzyme and incubated on a
638 thermal cycler for 12 min at 37°C followed by 30 min at 65°C. Adaptor ligated
639 libraries were prepared by adding 30 µL of ligation mix, 1 µL ligation enhancer (New
640 England BioLabs), 0.9 µL nuclease-free water (Ambion) and 0.1 µL duplexed
641 adapters to each well followed by incubation for 20 min at 20°C. Libraries were
642 purified and eluted by adding 65 µL of Ampure XP beads and 65 µL of TE buffer.
643 Libraries were amplified by adding 25 µL KAPA HiFi HotStart ReadyMix (KAPA
644 Biosystems) and 1 µL PE1.0 primer to 21.5 µL of the library. Each sample was
645 thermal-cycled as follows: 98 °C for 5 min, then 12 cycles of 98°C for 30 sec, 65°C
646 for 30 sec, 72°C for 1 min and finally 72°C for 5 min. Ampure beads were used to
647 purify amplified libraries using a 0.7:1 volumetric ratio of beads to library. Each
648 library was then eluted into 25 µL of nuclease-free water. Library concentrations

649 were adjusted to 2.4 nM and pooled, followed by sequencing on the Illumina
650 NovaSeq 6000 using 150 bp paired-end chemistry.
651
652 **Variant discovery and annotation**
653 In addition to the whole-genome sequencing of samples described above, sequence
654 data for 407 *S. mansoni* accessions (*39–41*) and one *S. rodhaini* accession (*40*)
655 were included in this study. Raw sequencing reads from all 682 accessions were
656 trimmed using BBDuk (https://jgi.doe.gov/data-and-tools/bbtools/bb-tools-user-
657 guide/) to remove low-quality bases and adapter sequences. Trimmed sequence
658 reads were aligned to the *S. mansoni* (SM_V9, WormBase ParaSite v16) (*69*)
659 reference genome using BWA mem (v.0.7.17) (*70*). PCR duplicates were marked
660 using PicardTools MarkDuplicates (as part of GATK v.4.2.0.0) (*71*). Variant calling
661 was performed per sample using GATK HaplotypeCaller (v.4.2.0.0) in gVCF mode,
662 retaining both variant and invariant sites. Individual gVCFs were merged using GATK
663 CombineGVCFs, and joint-call cohort genotyping was performed using GATK
664 GenotypeGVCFs. Variant sites with only single-nucleotide polymorphisms (SNPs)
665 were separated from indels and mixed sites (variant sites that had both SNPs and
666 indels called) using GATK SelectVariants. GATK VariantFiltration was used to filter
667 both groups independently. SNPs were retained if they met the following criteria:
668 QD ≥ 2.0, FS ≤ 60.0, MQ ≥ 40.0, MQRankSum ≥ −12.5, ReadPosRankSum ≥ −8.0,
669 SOR ≤ 3.0. Variant sites containing indels or mixed sites were retained if they met
670 the following criteria: QD ≥ 2.0, FS ≤ 200.0, ReadPosRankSum ≥ −20.0, SOR ≤ 10.0.
671
672 VCFtools (v.0.1.15) was used to exclude accessions with a high rate of variant site
673 missingness (missing genotype called at >5% of sites) and subsequently used to

674 remove sites where >10% of accessions had a missing genotype (*72*). This formed
675 the primary VCF file used for almost all analyses. For analyses of nucleotide
676 diversity and fixation index (F_{ST}), we produced a second filtered VCF file. We used
677 VCFtools to filter both variant and invariant sites with >80% missing variants,
678 enforced a minimum mean read depth of 5, a maximum mean read depth of 500,
679 removing variant sites found to be significantly out of Hardy-Weinberg equilibrium (p
680 < 0.001), and only retained SNPs. Functional annotation of SNPs and indels in the
681 primary VCF file was performed using SnpEff (v.5.0e) (*73*) with gene annotations
682 (v.9) downloaded from WormBase ParaSite (*74*) V17. Repetitive elements in the *S.*
683 *mansoni* assembly were annotated using RepeatModeler and RepeatMasker (*75*).
684

685 **Depth of coverage**

686 For each sample, the depth of read coverage was calculated in 2 kb windows along
687 each chromosome using bedtools coverage (v.2.30.0) (*76*).
688

689 **Sample relatedness**

690 We estimated pairwise relatedness between accessions from the same endemic
691 regions. We subsampled to only autosomal SNPs and ran NgsRelate (*77*) using
692 default parameters. As an additional line of evidence, we first used PLINK (v.2.0)
693 (*78*) to exclude SNPs found to be in strong linkage disequilibrium. The genome was
694 then scanned in sliding windows of 50 SNPs, increasing in steps of 10 SNPs and
695 SNPs within windows with squared correlation coefficients >0.2 were removed.
696 Using this filtered subset of SNPs, we performed pedigree reconstruction using
697 Sequoia (*79*). Pairwise relationships were first classified based on the coefficient of
698 kinship score (θ) calculated by NgsRelate. NgsRelate was first run on all 570 *S.*

699 *mansoni* samples to identify relationships between datasets or populations. After
700 confirming these relationships did not occur, NgsRelate was rerun on individual
701 populations from Southern Uganda, Northern Tanzania and Koome Islands.
702 Additionally, samples from Berger et al. (*39*) were excluded from these analyses due
703 to both highly elevated inbreeding coefficients in this dataset. Pairwise relationships
704 with $\theta > 0.354$ were classified as monozygotic twins, $0.354 > \theta \geq 0.177$ were
705 classified as first-degree relatives, $0.177 > \theta \geq 0.0884$ were classified as second-
706 degree relatives and $0.0884 > \theta \geq 0.0442$ were classified as third-degree relatives. In
707 addition, first-, second-, and third-degree relationships were only considered valid if
708 the maximum likelihood estimate of sharing 1 IBD allele (K_1) was greater than 0.05.
709 Instances where both NgsRelate and Sequoia identified the same first-degree
710 relationships were designated 'high-confidence' relationships. GGtern was used to
711 plot all three maximum likelihood estimates of sharing 0, 1 or 2 IBD alleles (K_0, K_1,
712 and K_2), and Circos (*80*) and Gephi (*81*) were used to visualise pairwise relationships
713 between different donors.
714
715 **Population genomic structure and diversity**
716 We removed variants found at minor allele frequencies < 0.05 and excluded all
717 variants found on the Z chromosome, W chromosome and mitochondrial genome.
718 We then removed all variants found within repetitive regions identified using
719 RepeatMasker and finally removed variants found to be in strong linkage
720 disequilibrium, as above. Principal component analysis was performed with the
721 remaining 188,923 autosomal SNPs using PLINK. Admixture analyses were
722 performed using ADMIXTURE (*82*) with K values (number of hypothetical ancestral
723 populations) ranging from 1 to 20, 10-fold cross-validation and standard error

724 estimation with 250 bootstraps. The lowest cross-validation error (CV) value was
725 found for K = 5 (Supplementary Fig. 13).
726
727 We used publicly-available scripts to convert all 188,923 autosomal SNPs into Phylip
728 format (https://github.com/edgardomortiz/vcf2phylip/vcf2phylip.py) and remove
729 invariant sites (https://github.com/btmartin721/raxml_ascbias/ascbias.py).
730 Phylogenomic inference was performed using IQ-TREE (*83*), using the best-fit
731 substitution model with ascertainment bias correction selected by ModelFinder
732 (GTR+F+ASC+R10) and 1000 ultrafast bootstraps. The resulting phylogeny was
733 visualised using ggtree (*84*).
734
735 pixy (v.1.2.3.beta1) (*85*) was used to calculate autosomal nucleotide diversity (π)
736 and the fixation index (F_{ST}) in 5 kb non-overlapping, sliding windows for each
737 population using the secondary (mixed variant and invariant sites) VCF. Negative F_{ST}
738 values were corrected to 0 before calculating genome-wide median values.
739 Watterson's estimator (Θ) was calculated using Scikit-allel (*86*). Effective population
740 size (N_e) was using a per-generation mutation rate (μ) of 8.1×10^{-9} (*40*) and the
741 following equation:
742 $$Ne = \Theta/4\mu$$
743 The coefficient of inbreeding (F) was calculated using VCFtools to assess per-
744 sample homozygosity. Comparisons of samples within and between study sites can
745 be found in Supplementary Fig. 14A-C.
746
747 **The impact of praziquantel treatment on population genomic diversity**

748 pixy (v.1.2.3.beta1) was used to calculate autosomal nucleotide diversity (π) in 5 kb
749 non-overlapping, sliding windows for each pre- and post-treatment population using
750 the secondary (mixed variant and invariant sites) VCF and including related
751 accessions (*85*).
752
753 **Structural variant genotyping and annotation**
754 Structural variants for each sample were detected using LUMPY (v.0.2.13) and
755 genotyped using SVTyper (v.0.7.0) as implemented in the Smoove (v.0.2.7) pipeline
756 (https://github.com/brentp/smoove) (*87*, *88*). Using this pipeline, we first performed
757 single-sample calling using the BWA-aligned reads to the *S. mansoni* reference
758 genome. This was followed by merging called variants and sample-wise re-
759 genotyping across all 570 *S. mansoni* accessions. Structural variants intersecting
760 coding regions were annotated using the reference GFF file. We then filtered
761 variants based on the Smoove author's recommendations, where heterozygous calls
762 with MSHQ>=3, deletions with DHFFC>=0.7 and duplications with DHFFC<=1.25
763 were excluded. Due to inconsistent coverage and whole-genome amplification of the
764 original libraries, all accessions from Berger et al. (*39*) were excluded from structural
765 variant analyses after genotyping.
766
767 **Inference of demographic history**
768 We ran SMC++ (v.1.15.2) (*89*) on each autosome using a per-generation mutation
769 rate of 8.1×10^{-9} and a generation time of 85 days. For Southern Ugandan, Koome
770 Island, Northern Tanzanian, and Eastern Ugandan populations, we randomly subset
771 them down to n = 12 unrelated accessions, providing replicates where populations

772 had more than 24 accessions. For all other populations, only single accessions were
773 analysed.
774
775 **Screening for recent admixture**
776 Analysis of passaged laboratory strains also identified a single probable *S. mansoni-*
777 *S.rodhaini* hybrid (RZ0001), which displayed high heterozygosity, intermediate
778 admixture proportions and intermediate phylogenetic positioning, consistent with an
779 early-generation (F_1 - F_3) hybrid, this sample was excluded from further analyses
780 (Supplementary Fig. 15; Supplementary Data 2) (*90*, *91*).
781
782 **Analysis of candidate praziquantel resistance genes**
783 We inspected SnpEff annotated variants within the candidate praziquantel resistance
784 gene (*Smp_24790*), focusing on isoform 5 (*Smp_246790.5* in the v9 annotation), the
785 only full-length isoform containing the predicted binding site. Frequencies of
786 functionally impactful mutations were calculated using only Lake Victoria accessions.
787 The maximum-likelihood phylogeny produced previously was annotated to highlight
788 accessions containing specifically functionally impactful mutations. We excluded a
789 single indel, p.Met1fs, which was a frameshift variant and a short repeat from the
790 analysis; for completeness, information on this variant is still reported in
791 Supplementary Data 7,9,10.
792
793 **Ca^{2+} reporter assays**
794 Ca^{2+} imaging assays were performed using a Fluorescence Imaging Plate Reader
795 (FLIPR^{TETRA}, Molecular Devices). HEK293 cells (naïve or transfected with specific
796 $TRPM_{PZQ}$ variants) were seeded (20,000 cells/well) in a black-walled clear-bottomed

797 poly-d-lysine coated 384-well plate (Corning) in DMEM growth media supplemented
798 with 10% FBS. This medium was removed after 24hrs, and the cells were loaded
799 with a fluorescent Ca^{2+} indicator (Fluo-4 NW dye, Invitrogen) by incubation (20 µL
800 per well, 1 h at 37°C) in Hanks' balanced salt solution (HBSS) assay buffer
801 containing probenecid (2.5 mM) and HEPES (20mM). Dilutions of praziquantel
802 (Sigma) were prepared in this same buffer, but without probenecid and dye, in flat
803 shape 384-well plates (Greiner Bio-one, Germany). The Ca^{2+} reporter assay was
804 performed at room temperature by monitoring fluorescence (raw fluorescence units)
805 before (basal, 20s) and after the addition of praziquantel (an additional 250s). For
806 quantitative analyses, peak fluorescence in each well was normalised to the maximal
807 response of the reference channel sequence and concentration-response curves
808 were plotted using the sigmoidal dose-response function in Origin.
809
810

811 **List of Supplementary Materials**

812 Supplementary Data 1 to 14
813 Supplementary Figs 1 to 15

814 **References**

815 1. Control of Neglected Tropical Diseases (NTD) Guidelines Review Committee,
816 "WHO Guideline on control and elimination of human schistosomiasis" (World
817 Health Organization, 2022).

818 2. N. C. Lo, F. S. M. Bezerra, D. G. Colley, F. M. Fleming, M. Homeida, N.
819 Kabatereine, F. M. Kabole, C. H. King, M. A. Mafe, N. Midzi, F. Mutapi, J. R.
820 Mwanga, R. M. R. Ramzy, F. Satrija, J. R. Stothard, M. S. Traoré, J. P. Webster,
821 J. Utzinger, X.-N. Zhou, A. Danso-Appiah, P. Eusebi, E. S. Loker, C. O. Obonyo,
822 R. Quansah, S. Liang, M. Vaillant, M. H. Murad, P. Hagan, A. Garba, Review of
823 2022 WHO guidelines on the control and elimination of schistosomiasis. *Lancet*
824 *Infect. Dis.* **22**, e327–e335 (2022).

3. D. G. Colley, A. L. Bustinduy, W. E. Secor, C. H. King, Human schistosomiasis. *Lancet* **383**, 2253–2264 (2014).

4. WHO Expert Committee on the Control of Schistosomiasis, “Prevention and control of schistosomiasis and soil-transmitted helminthiasis : report of a WHO expert committee” (World Health Organ Tech Rep Ser., 2002); http://apps.who.int/iris/handle/10665/42588.

5. J. P. Webster, D. H. Molyneux, P. J. Hotez, A. Fenwick, The contribution of mass drug administration to global health: past, present and future. *Philos. Trans. R. Soc. Lond. B Biol. Sci.* **369**, 20130434 (2014).

6. World Health Organization, Schistosomiasis and soil-transmitted helminthiases: progress report, 2020 - Schistosomiase et géohelminthiases: rapport de situation, 2020. *Weekly Epidemiological Record* **96**, 585–595 (2021).

7. A. K. Deol, F. M. Fleming, B. Calvo-Urbano, M. Walker, V. Bucumi, I. Gnandou, E. M. Tukahebwa, S. Jemu, U. J. Mwingira, A. Alkohlani, M. Traoré, E. Ruberanziza, S. Touré, M.-G. Basáñez, M. D. French, J. P. Webster, Schistosomiasis - assessing progress toward the 2020 and 2025 global goals. *N. Engl. J. Med.* **381**, 2519–2528 (2019).

8. C. Kokaliaris, A. Garba, M. Matuska, R. N. Bronzan, D. G. Colley, A. M. Dorkenoo, U. F. Ekpo, F. M. Fleming, M. D. French, A. Kabore, J. B. Mbonigaba, N. Midzi, P. N. M. Mwinzi, E. K. N’Goran, M. R. Polo, M. Sacko, L.-A. Tchuem Tchuenté, E. M. Tukahebwa, P. A. Uvon, G. Yang, L. Wiesner, Y. Zhang, J. Utzinger, P. Vounatsou, Effect of preventive chemotherapy with praziquantel on schistosomiasis among school-aged children in sub-Saharan Africa: a spatiotemporal modelling study. *Lancet Infect. Dis.* **22**, 136–149 (2022).

9. World Health Organization, “A road map for neglected tropical diseases 2021–2030” (World Health Organization, 2020); https://www.who.int/neglected_diseases/Ending-the-neglect-to-attain-the-SDGs--NTD-Roadmap.pdf.

10. N. B. Kabatereine, S. Brooker, A. Koukounari, F. Kazibwe, E. M. Tukahebwa, F. M. Fleming, Y. Zhang, J. P. Webster, J. R. Stothard, A. Fenwick, Impact of a national helminth control programme on infection and morbidity in Ugandan schoolchildren. *Bull. World Health Organ.* **85**, 91–99 (2007).

11. R. N. Bronzan, A. M. Dorkenoo, Y. M. Agbo, W. Halatoko, Y. Layibo, P. Adjeloh, M. Teko, E. Sossou, K. Yakpa, M. Tchalim, G. Datagni, A. Seim, K. S. Sognikin, Impact of community-based integrated mass drug administration on schistosomiasis and soil-transmitted helminth prevalence in Togo. *PLoS Negl. Trop. Dis.* **12**, e0006551 (2018).

12. P. A. Mawa, J. Kincaid-Smith, E. M. Tukahebwa, J. P. Webster, S. Wilson, Schistosomiasis morbidity hotspots: roles of the human host, the parasite and their interface in the development of severe morbidity. *Front. Immunol.* **12**, 751 (2021).

13. M. W. Mutuku, M. R. Laidemitt, B. R. Beechler, I. N. Mwangi, F. O. Otiato, E. L. Agola, H. Ochanda, B. Kamel, G. M. Mkoji, M. L. Steinauer, Others, A search for snail-related answers to explain differences in response of *Schistosoma mansoni* to praziquantel treatment among responding and persistent hotspot villages along the Kenyan shore of Lake Victoria. *Am. J. Trop. Med. Hyg.* **101**, 65–77 (2019).

14. N. Kittur, C. H. King, C. H. Campbell Jr, S. Kinung'hi, P. N. M. Mwinzi, D. M. S. Karanja, E. K. N'Goran, A. E. Phillips, P. H. Gazzinelli-Guimaraes, A. Olsen, Others, Persistent hotspots in schistosomiasis consortium for operational research and evaluation studies for gaining and sustaining control of schistosomiasis after four years of mass drug administration of praziquantel. *Am. J. Trop. Med. Hyg.* **101**, 617–627 (2019).

15. R. M. Lim, T. M. Arme, A. B. Pedersen, J. P. Webster, P. H. L. Lamberton, Defining schistosomiasis hotspots based on literature and shareholder interviews. *Trends Parasitol.* **39**, 1032–1049 (2023).

16. L. Mari, M. Ciddio, R. Casagrandi, J. Perez-Saez, E. Bertuzzo, A. Rinaldo, S. H. Sokolow, G. A. De Leo, M. Gatto, Heterogeneity in schistosomiasis transmission dynamics. *J. Theor. Biol.* **432**, 87–99 (2017).

17. L. Meurs, M. Mbow, N. Boon, F. van den Broeck, K. Vereecken, T. N. Dièye, E. Abatih, T. Huyse, S. Mboup, K. Polman, Micro-geographical heterogeneity in *Schistosoma mansoni* and *S. haematobium* infection and morbidity in a co-endemic community in northern Senegal. *PLoS Negl. Trop. Dis.* **7**, e2608 (2013).

18. M. Aemero, J. Boissier, D. Climent, H. Moné, G. Mouahid, N. Berhe, B. Erko, Genetic diversity, multiplicity of infection and population structure of *Schistosoma mansoni* isolates from human hosts in Ethiopia. *BMC Genet.* **16**, 137 (2015).

19. S. D. Melman, M. L. Steinauer, C. Cunningham, L. S. Kubatko, I. N. Mwangi, N. B. Wynn, M. W. Mutuku, D. M. S. Karanja, D. G. Colley, C. L. Black, W. E. Secor, G. M. Mkoji, E. S. Loker, Reduced Susceptibility to Praziquantel among Naturally Occurring Kenyan Isolates of *Schistosoma mansoni*. *PLoS Negl. Trop. Dis.* **3**, e504 (2009).

20. T. Crellen, M. Walker, P. H. L. Lamberton, N. B. Kabatereine, E. M. Tukahebwa, J. A. Cotton, J. P. Webster, Reduced Efficacy of Praziquantel

900 Against *Schistosoma mansoni* Is Associated with Multiple Rounds of Mass Drug
901 Administration. *Clin. Infect. Dis.* **63**, 1151–1159 (2016).

902 21. F. F. Stelma, I. Talla, S. Sow, A. Kongs, M. Niang, K. Polman, A. M.
903 Deelder, B. Gryseels, Efficacy and side effects of praziquantel in an epidemic
904 focus of *Schistosoma mansoni*. *Am. J. Trop. Med. Hyg.* **53**, 167–170 (1995).

905 22. A. E. Lelo, D. N. Mburu, G. N. Magoma, B. N. Mungai, J. H. Kihara, I.
906 N. Mwangi, G. M. Maina, J. M. Kinuthia, M. W. Mutuku, E. S. Loker, G. M. Mkoji,
907 M. L. Steinauer, No apparent reduction in schistosome burden or genetic
908 diversity following four years of school-based mass drug administration in Mwea,
909 central Kenya, a heavy transmission area. *PLoS Negl. Trop. Dis.* **8**, e3221
910 (2014).

911 23. T. Huyse, F. Van den Broeck, T. Jombart, B. L. Webster, O. Diaw, F. A.
912 M. Volckaert, F. Balloux, D. Rollinson, K. Polman, Regular treatments of
913 praziquantel do not impact on the genetic make-up of *Schistosoma mansoni* in
914 Northern Senegal. *Infect. Genet. Evol.* **18**, 100–105 (2013).

915 24. R. E. Blanton, W. A. Blank, J. M. Costa, T. M. Carmo, E. A. Reis, L. K.
916 Silva, L. M. Barbosa, M. R. Test, M. G. Reis, *Schistosoma mansoni* population
917 structure and persistence after praziquantel treatment in two villages of Bahia,
918 Brazil. *Int. J. Parasitol.* **41**, 1093–1099 (2011).

919 25. C. L. Faust, M. Crotti, A. Moses, D. Oguttu, A. Wamboko, M. Adriko, E.
920 K. Adekanle, N. Kabatereine, E. M. Tukahebwa, A. J. Norton, C. M. Gower, J. P.
921 Webster, P. H. L. Lamberton, Two-year longitudinal survey reveals high genetic
922 diversity of *Schistosoma mansoni* with adult worms surviving praziquantel
923 treatment at the start of mass drug administration in Uganda. *Parasit. Vectors*
924 **12**, 607 (2019).

925 26. P. G. Fallon, M. J. Doenhoff, Drug-resistant schistosomiasis: resistance
926 to praziquantel and oxamniquine induced in *Schistosoma mansoni* in mice is
927 drug specific. *Am. J. Trop. Med. Hyg.* **51**, 83–88 (1994).

928 27. F. F. B. Couto, P. M. Z. Coelho, N. Araújo, J. R. Kusel, N. Katz, L. K.
929 Jannotti-Passos, A. C. A. Mattos, *Schistosoma mansoni*: a method for inducing
930 resistance to praziquantel using infected *Biomphalaria glabrata* snails. *Mem.*
931 *Inst. Oswaldo Cruz* **106**, 153–157 (2011).

932 28. I. N. Mwangi, M. C. Sanchez, G. M. Mkoji, L. E. Agola, S. M. Runo, P.
933 M. Cupit, C. Cunningham, Praziquantel sensitivity of Kenyan *Schistosoma*
934 *mansoni* isolates and the generation of a laboratory strain with reduced
935 susceptibility to the drug. *Int. J. Parasitol. Drugs Drug Resist.* **4**, 296–300 (2014).

936 29. P. H. L. Lamberton, C. L. Faust, J. P. Webster, Praziquantel decreases

937 fecundity in *Schistosoma mansoni* adult worms that survive treatment: evidence
938 from a laboratory life-history trade-offs selection study. *Infect Dis Poverty* **6**, 110
939 (2017).

940 30. M. Fukushige, M. Chase-Topping, M. E. J. Woolhouse, F. Mutapi,
941 Efficacy of praziquantel has been maintained over four decades (from 1977 to
942 2018): A systematic review and meta-analysis of factors influence its efficacy.
943 *PLoS Negl. Trop. Dis.* **15**, e0009189 (2021).

944 31. H. Rose, L. Rinaldi, A. Bosco, F. Mavrot, T. de Waal, P. Skuce, J.
945 Charlier, P. R. Torgerson, H. Hertzberg, G. Hendrickx, J. Vercruysse, E. R.
946 Morgan, Widespread anthelmintic resistance in European farmed ruminants: a
947 systematic review. *Vet. Rec.* **176**, 546 (2015).

948 32. R. M. Kaplan, A. N. Vidyashankar, An inconvenient truth: global
949 worming and anthelmintic resistance. *Vet. Parasitol.* **186**, 70–78 (2012).

950 33. A. E. Schwab, D. A. Boakye, D. Kyelem, R. K. Prichard, Detection of
951 benzimidazole resistance-associated mutations in the filarial nematode
952 *Wuchereria bancrofti* and evidence for selection by albendazole and ivermectin
953 combination treatment. *Am. J. Trop. Med. Hyg.* **73**, 234–238 (2005).

954 34. S. R. Doyle, R. Laing, D. Bartley, A. Morrison, N. Holroyd, K. Maitland,
955 A. Antonopoulos, U. Chaudhry, I. Flis, S. Howell, J. McIntyre, J. S. Gilleard, A.
956 Tait, B. Mable, R. Kaplan, N. Sargison, C. Britton, M. Berriman, E. Devaney, J.
957 A. Cotton, Genomic landscape of drug response reveals mediators of
958 anthelmintic resistance. *Cell Rep.* **41**, 111522 (2022).

959 35. S.-K. Park, G. S. Gunaratne, E. G. Chulkov, F. Moehring, P. McCusker,
960 P. I. Dosa, J. D. Chan, C. L. Stucky, J. S. Marchant, The anthelmintic drug
961 praziquantel activates a schistosome transient receptor potential channel. *J.*
962 *Biol. Chem.* **294** (2019).

963 36. S.-K. Park, L. Friedrich, N. A. Yahya, C. M. Rohr, E. G. Chulkov, D.
964 Maillard, F. Rippmann, T. Spangenberg, J. S. Marchant, Mechanism of
965 praziquantel action at a parasitic flatworm ion channel. *Sci. Transl. Med.* **13**,
966 eabj5832 (2021).

967 37. W. Le Clec'h, F. D. Chevalier, A. C. A. Mattos, A. Strickland, R. Diaz,
968 M. McDew-White, C. M. Rohr, S. Kinung'hi, F. Allan, B. L. Webster, J. P.
969 Webster, A. M. Emery, D. Rollinson, A. G. Djirmay, K. M. Al Mashikhi, S. Al
970 Yafae, M. A. Idris, H. Moné, G. Mouahid, P. LoVerde, J. S. Marchant, T. J. C.
971 Anderson, Genetic analysis of praziquantel response in schistosome parasites
972 implicates a transient receptor potential channel. *Sci. Transl. Med.* **13**, eabj9114
973 (2021).

38. J. S. Marchant, Progress interrogating TRPMPZQ as the target of praziquantel. *PLoS Negl. Trop. Dis.* **18**, e0011929 (2024).

39. D. J. Berger, T. Crellen, P. H. L. Lamberton, F. Allan, A. Tracey, J. D. Noonan, N. B. Kabatereine, E. M. Tukahebwa, M. Adriko, N. Holroyd, J. P. Webster, M. Berriman, J. A. Cotton, Whole-genome sequencing of *Schistosoma mansoni* reveals extensive diversity with limited selection despite mass drug administration. *Nat. Commun.* **12**, 4776 (2021).

40. T. Crellen, F. Allan, S. David, C. Durrant, T. Huckvale, N. Holroyd, A. M. Emery, D. Rollinson, D. M. Aanensen, M. Berriman, J. P. Webster, J. A. Cotton, Whole genome resequencing of the human parasite *Schistosoma mansoni* reveals population history and effects of selection. *Sci. Rep.* **6**, 1–13 (2016).

41. T. J. Vianney, D. J. Berger, S. R. Doyle, G. Sankaranarayanan, J. Serubanja, P. K. Nakawungu, F. Besigye, R. E. Sanya, N. Holroyd, F. Allan, E. L. Webb, A. M. Elliott, M. Berriman, J. A. Cotton, Genome-wide analysis of *Schistosoma mansoni* reveals limited population structure and possible praziquantel drug selection pressure within Ugandan hot-spot communities. *PLoS Negl. Trop. Dis.* **16**, e0010188 (2022).

42. F. D. Chevalier, W. Le Clec'h, M. Berriman, T. J. C. Anderson, A single locus determines praziquantel response in *Schistosoma mansoni*. *Antimicrob. Agents Chemother.* **68**, e0143223 (2024).

43. R. N. Platt, W. Le Clec'h, F. D. Chevalier, M. McDew-White, P. T. LoVerde, R. de Assis R, G. Oliveira, S. Kinung'hi, A. G. Djirmay, M. L. Steinauer, A. Gouvras, M. Rabone, F. Allan, B. L. Webster, J. P. Webster, A. M. Emery, D. Rollinson, T. J. C. Anderson, Genomic analysis of a parasite invasion: colonization of the Americas by the blood fluke, *Schistosoma mansoni*. *Mol. Ecol.* **31**, 2242–2263 (2021).

44. S. Summers, T. Bhattacharyya, F. Allan, R. J. Stothard, A. Edielu, B. L. Webster, M. A. Miles, B. Al., A review of the genetic determinants of praziquantel resistance in *Schistosoma mansoni*: Is praziquantel and intestinal schistosomiasis a perfect match? *Front. Trop. Dis.* **3** (2022).

45. Z.-Z. Mei, R. Xia, D. J. Beech, L.-H. Jiang, Intracellular coiled-coil domain engaged in subunit interaction and assembly of melastatin-related transient receptor potential channel 2. *J. Biol. Chem.* **281**, 38748–38756 (2006).

46. Y. Yin, S. C. Le, A. L. Hsu, M. J. Borgnia, H. Yang, S.-Y. Lee, Structural basis of cooling agent and lipid sensing by the cold-activated TRPM8 channel. *Science* **363**, eaav9334 (2019).

1011 47. L. E. Agola, M. L. Steinauer, D. N. Mburu, B. N. Mungai, I. N. Mwangi,
1012 G. N. Magoma, E. S. Loker, G. M. Mkoji, Genetic diversity and population
1013 structure of *Schistosoma mansoni* within human infrapopulations in Mwea,
1014 central Kenya assessed by microsatellite markers. *Acta Trop.* **111**, 219–225
1015 (2009).

1016 48. M. I. Neves, J. P. Webster, M. Walker, Estimating helminth burdens
1017 using sibship reconstruction. *Parasit. Vectors* **12**, 441 (2019).

1018 49. F. D. Chevalier, W. Le Clec'h, M. McDew-White, V. Menon, M. A.
1019 Guzman, S. P. Holloway, X. Cao, A. B. Taylor, S. Kinung'hi, A. N. Gouvras, B. L.
1020 Webster, J. P. Webster, A. M. Emery, D. Rollinson, A. Garba Djirmay, K. M. Al
1021 Mashikhi, S. Al Yafae, M. A. Idris, H. Moné, G. Mouahid, P. J. Hart, P. T.
1022 LoVerde, T. J. C. Anderson, Oxamniquine resistance alleles are widespread in
1023 Old World *Schistosoma mansoni* and predate drug deployment. *PLoS Pathog.*
1024 **15**, e1007881 (2019).

1025 50. F. D. Chevalier, W. Le Clec'h, N. Eng, A. R. Rugel, R. R. de Assis, G.
1026 Oliveira, S. P. Holloway, X. Cao, P. John Hart, P. T. LoVerde, T. J. C. Anderson,
1027 Independent origins of loss-of-function mutations conferring oxamniquine
1028 resistance in a Brazilian schistosome population. *Int. J. Parasitol.* **46**, 417–424
1029 (2016).

1030 51. A. Jacquard, Logique du calcul des coefficients d'identité entre deux
1031 individus. *Population* **21**, 751–776 (1966).

1032 52. J. E. Hodgkinson, R. M. Kaplan, F. Kenyon, E. R. Morgan, A. W. Park,
1033 S. Paterson, S. A. Babayan, N. J. Beesley, C. Britton, U. Chaudhry, S. R. Doyle,
1034 V. O. Ezenwa, A. Fenton, S. B. Howell, R. Laing, B. K. Mable, L. Matthews, J.
1035 McIntyre, C. E. Milne, T. A. Morrison, J. C. Prentice, N. D. Sargison, D. J. L.
1036 Williams, A. J. Wolstenholme, E. Devaney, Refugia and anthelmintic resistance:
1037 Concepts and challenges. *Int. J. Parasitol. Drugs Drug Resist.* **10**, 51–57 (2019).

1038 53. D. M. Leathwick, S. Ganesh, T. S. Waghorn, Evidence for reversion
1039 towards anthelmintic susceptibility in *Teladorsagia circumcincta* in response to
1040 resistance management programmes. *Int. J. Parasitol. Drugs Drug Resist.* **5**, 9–
1041 15 (2015).

1042 54. F. Kenyon, A. W. Greer, G. C. Coles, G. Cringoli, E. Papadopoulos, J.
1043 Cabaret, B. Berrag, M. Varady, J. A. Van Wyk, E. Thomas, J. Vercruysse, F.
1044 Jackson, The role of targeted selective treatments in the development of refugia-
1045 based approaches to the control of gastrointestinal nematodes of small
1046 ruminants. *Vet. Parasitol.* **164**, 3–11 (2009).

1047 55. B. Gryseels, S. J. De Vlas, Worm burdens in schistosome infections.
1048 *Parasitol. Today* **12**, 115–119 (1996).

1049 56. M. I. Neves, C. M. Gower, J. P. Webster, M. Walker, Revisiting density-
1050 dependent fecundity in schistosomes using sibship reconstruction. *PLoS Negl.*
1051 *Trop. Dis.* **15**, e0009396 (2021).

1052 57. N. Katz, A. Chaves, J. Pellegrino, A simple device for quantitative stool
1053 thick-smear technique in *Schistosoma mansoni*. *Rev. Inst. Med. Trop. Sao Paulo*
1054 **14**, 397–400 (1972).

1055 58. R. J. Pitchford, P. S. Visser, A simple and rapid technique for
1056 quantitative estimation of helminth eggs in human and animal excreta with
1057 special reference to *Schistosoma sp. Trans. R. Soc. Trop. Med. Hyg.* **69**, 318–
1058 322 (1975).

1059 59. A. M. Emery, F. E. Allan, M. E. Rabone, D. Rollinson, Schistosomiasis
1060 collection at NHM (SCAN). *Parasit. Vectors* **5**, 1 (2012).

1061 60. C. M. Gower, J. Shrivastava, P. H. L. Lamberton, D. Rollinson, B. L.
1062 Webster, A. Emery, N. B. Kabatereine, J. P. Webster, Development and
1063 application of an ethically and epidemiologically advantageous assay for the
1064 multi-locus microsatellite analysis of *Schistosoma mansoni*. *Parasitology* **134**,
1065 523–536 (2007).

1066 61. M. Adriko, C. J. Standley, B. Tinkitina, G. Mwesigwa, T. K. Kristensen,
1067 J. R. Stothard, N. B. Kabatereine, Compatibility of Ugandan *Schistosoma*
1068 *mansoni* isolates with *Biomphalaria* snail species from Lake Albert and Lake
1069 Victoria. *Acta Trop.* **128**, 303–308 (2013).

1070 62. A. N. Gouvras, F. Allan, S. Kinung'hi, M. Rabone, A. Emery, T. Angelo,
1071 T. Pennance, B. Webster, H. Nagai, D. Rollinson, Longitudinal survey on the
1072 distribution of *Biomphalaria sudanica* and *B. choanomophala* in Mwanza region,
1073 on the shores of Lake Victoria, Tanzania: implications for schistosomiasis
1074 transmission and control. *Parasit. Vectors* **10** (2017).

1075 63. A. E. Ezeamama, C.-L. He, Y. Shen, X.-P. Yin, S. C. Binder, C. H.
1076 Campbell, S. Rathbun, C. C. Whalen, E. K. N'Goran, J. Utzinger, A. Olsen, P.
1077 Magnussen, S. Kinung'hi, A. Fenwick, A. Phillips, J. Ferro, D. M. S. Karanja, P.
1078 N. M. Mwinzi, S. Montgomery, W. Evan Secor, A. Hamidou, A. Garba, C. H.
1079 King, D. G. Colley, Gaining and sustaining schistosomiasis control: study
1080 protocol and baseline data prior to different treatment strategies in five African
1081 countries. *BMC Infectious Diseases* **16** (2016).

1082 64. P. G. Fallon, M. J. Doenhoff, A. Capron, R. F. Sturrock, M. Niang,
1083 Short Report: Diminished Susceptibility to Praziquantel in a Senegal Isolate of
1084 *Schistosoma mansoni*. *Am J Trop Med Hyg* **53**, 61–62 (1995).

1085 65. P. G. Fallon, J. S. Mubarak, R. E. Fookes, M. Niang, A. E. Butterworth,

1086 R. F. Sturrock, M. J. Doenhoff, *Schistosoma mansoni*: maturation rate and drug
1087 susceptibility of different geographic isolates. *Exp. Parasitol.* **86**, 29–36 (1997).

1088 66. L. Moore, D. Leongamornlert, T. H. H. Coorens, M. A. Sanders, P.
1089 Ellis, S. C. Dentro, K. J. Dawson, T. Butler, R. Rahbari, T. J. Mitchell, F. Maura,
1090 J. Nangalia, P. S. Tarpey, S. F. Brunner, H. Lee-Six, Y. Hooks, S. Moody, K. T.
1091 Mahbubani, M. Jimenez-Linan, J. J. Brosens, C. A. Iacobuzio-Donahue, I.
1092 Martincorena, K. Saeb-Parsy, P. J. Campbell, M. R. Stratton, The mutational
1093 landscape of normal human endometrial epithelium. *Nature* **580**, 640–646
1094 (2020).

1095 67. S. R. Doyle, G. Sankaranarayanan, F. Allan, D. Berger, P. D. Jimenez
1096 Castro, J. B. Collins, T. Crellen, M. A. Duque-Correa, P. Ellis, T. G. Jaleta, R.
1097 Laing, K. Maitland, C. McCarthy, T. Moundai, B. Softley, E. Thiele, P. T. Ouakou,
1098 J. V. Tushabe, J. P. Webster, A. J. Weiss, J. Lok, E. Devaney, R. M. Kaplan, J.
1099 A. Cotton, M. Berriman, N. Holroyd, Evaluation of DNA Extraction Methods on
1100 Individual Helminth Egg and Larval Stages for Whole-Genome Sequencing.
1101 *Front. Genet.* **10**, 826 (2019).

1102 68. H. Lee-Six, P. Ellis, R. J. Osborne, M. A. Sanders, L. Moore, N.
1103 Georgakopoulos, F. Torrente, A. Noorani, M. Goddard, P. Robinson, T. H. H.
1104 Coorens, L. O'Neill, C. Alder, J. Wang, R. C. Fitzgerald, M. Zilbauer, N.
1105 Coleman, K. Saeb-Parsy, I. Martincorena, P. J. Campbell, M. R. Stratton, The
1106 landscape of somatic mutation in normal colorectal epithelial cells. *Nature* **574**,
1107 532–537 (2019).

1108 69. S. K. Buddenborg, A. Tracey, D. J. Berger, Z. Lu, S. R. Doyle, B. Fu, F.
1109 Yang, A. J. Reid, F. H. Rodgers, G. Rinaldi, G. Sankaranarayanan, U. Böhme,
1110 N. Holroyd, M. Berriman, Assembled chromosomes of the blood fluke
1111 *Schistosoma mansoni* provide insight into the evolution of its ZW sex-
1112 determination system. *bioRxiv* (2021).

1113 70. H. Li, Aligning sequence reads, clone sequences and assembly contigs
1114 with BWA-MEM, *arXiv [q-bio.GN]* (2013). http://arxiv.org/abs/1303.3997.

1115 71. A. McKenna, M. Hanna, E. Banks, A. Sivachenko, K. Cibulskis, A.
1116 Kernytsky, K. Garimella, D. Altshuler, S. Gabriel, M. Daly, M. A. DePristo, The
1117 Genome Analysis Toolkit: a MapReduce framework for analyzing next-
1118 generation DNA sequencing data. *Genome Res.* **20**, 1297–1303 (2010).

1119 72. P. Danecek, A. Auton, G. Abecasis, C. A. Albers, E. Banks, M. A.
1120 DePristo, R. E. Handsaker, G. Lunter, G. T. Marth, S. T. Sherry, G. McVean, R.
1121 Durbin, 1000 Genomes Project Analysis Group, The variant call format and
1122 VCFtools. *Bioinformatics* **27**, 2156–2158 (2011).

1123 73. P. Cingolani, A. Platts, L. L. Wang, M. Coon, T. Nguyen, L. Wang, S. J.

Land, X. Lu, D. M. Ruden, A program for annotating and predicting the effects of single nucleotide polymorphisms, SnpEff. *Fly* **6**, 80–92 (2012).

74. K. L. Howe, B. J. Bolt, M. Shafie, P. Kersey, M. Berriman, WormBase ParaSite - a comprehensive resource for helminth genomics. *Mol. Biochem. Parasitol.* **215**, 2–10 (2017).

75. A. F. A. Smit, R. Hubley, P. Green, *RepeatMasker Open-4.0. 2013-2015* (2015; http://www.repeatmasker.org).

76. A. R. Quinlan, I. M. Hall, BEDTools: a flexible suite of utilities for comparing genomic features. *Bioinformatics* **26**, 841–842 (2010).

77. K. Hanghøj, I. Moltke, P. A. Andersen, A. Manica, T. S. Korneliussen, Fast and accurate relatedness estimation from high-throughput sequencing data in the presence of inbreeding. *GigaScience* **8**, giz034 (2019).

78. C. C. Chang, C. C. Chow, L. C. Tellier, S. Vattikuti, S. M. Purcell, J. J. Lee, Second-generation PLINK: rising to the challenge of larger and richer datasets. *Gigascience* **4**, 7 (2015).

79. J. Huisman, Pedigree reconstruction from SNP data: parentage assignment, sibship clustering and beyond. *Mol. Ecol. Resour.* **17**, 1009–1024 (2017).

80. M. Krzywinski, J. Schein, I. Birol, J. Connors, R. Gascoyne, D. Horsman, S. J. Jones, M. A. Marra, Circos: an information aesthetic for comparative genomics. *Genome Res.* **19**, 1639–1645 (2009).

81. M. Bastian, S. Heymann, M. Jacomy, Gephi: an open source software for exploring and manipulating networks. *Proceedings of the International AAAI Conference on Web and Social Media* **3**, 361–362 (2009).

82. D. H. Alexander, J. Novembre, K. Lange, Fast model-based estimation of ancestry in unrelated individuals. *Genome Res.* **19**, 1655–1664 (2009).

83. B. Q. Minh, H. A. Schmidt, O. Chernomor, D. Schrempf, M. D. Woodhams, A. von Haeseler, R. Lanfear, IQ-TREE 2: New Models and Efficient Methods for Phylogenetic Inference in the Genomic Era. *Mol. Biol. Evol.* **37**, 1530–1534 (2020).

84. G. Yu, D. K. Smith, H. Zhu, Y. Guan, T. T.-Y. Lam, ggtree : an r package for visualization and annotation of phylogenetic trees with their covariates and other associated data. *Methods Ecol. Evol.* **8**, 28–36 (2017).

85. K. L. Korunes, K. Samuk, pixy: Unbiased estimation of nucleotide diversity and divergence in the presence of missing data. *Mol. Ecol. Resour.* **21**,

1359–1368 (2021).

86. A. Miles, P. io Bot, M. F. Rodrigues, P. Ralph, N. Harding, R. Pisupati, S. Rae, *Cggh/scikit-Allel: v1.3.1* (2020; https://zenodo.org/record/3935797).

87. R. M. Layer, C. Chiang, A. R. Quinlan, I. M. Hall, LUMPY: a probabilistic framework for structural variant discovery. *Genome Biol.* **15**, R84 (2014).

88. C. Chiang, R. M. Layer, G. G. Faust, M. R. Lindberg, D. B. Rose, E. P. Garrison, G. T. Marth, A. R. Quinlan, I. M. Hall, SpeedSeq: ultra-fast personal genome analysis and interpretation. *Nat. Methods* **12**, 966–968 (2015).

89. J. Terhorst, J. A. Kamm, Y. S. Song, Robust and scalable inference of population history from hundreds of unphased whole genomes. *Nat. Genet.* **49**, 303–309 (2017).

90. R. N. Platt, M. McDew-White, W. Le Clec'h, F. D. Chevalier, F. Allan, A. M. Emery, A. Garba, A. A. Hamidou, S. M. Ame, J. P. Webster, D. Rollinson, B. L. Webster, T. J. C. Anderson, Ancient Hybridization and Adaptive Introgression of an Invadolysin Gene in Schistosome Parasites. *Mol. Biol. Evol.* **36**, 2127–2142 (2019).

91. D. J. Berger, E. Léger, G. Sankaranarayanan, M. Sène, N. D. Diouf, M. Rabone, A. Emery, F. Allan, J. A. Cotton, M. Berriman, J. P. Webster, Genomic evidence of contemporary hybridization between *Schistosoma* species. *PLoS Pathog.* **18**, e1010706 (2022).

Acknowledgements

We would like to thank all the technicians, nurses and drivers who supported sample collections, including (but not exclusive to) Moses Arinaitwe, Aida Wamboko, Annet Enzaru, Andrina Nankasi, Aaron Atuhaire and Fiddi Rugigana from the Vector Control Division, Ugandan Ministry of Health, Uganda, and John Igogote, Honest Nagai, and Revocatus Alphonce from the National Institute for Medical Research, Tanzania. We would also like to thank the teachers from the schools we visited for their assistance and cooperation, the officials in the Health and Education Departments in districts of Mayuge (Uganda), and Alan Fenwick and Wendy Harrison of the Schistosomiasis Control Initiative (renamed Unlimit Health) for their help organising and funding the Ugandan fieldwork. Finally, we thank all the children recruited into this study and their parents and teachers for their cooperation.

Funding

Funding was via core funding of the Wellcome Sanger Institute (Wellcome grant 206194; PI: MB). Ugandan sampling was supported within the remit of Schistosomiasis Control Initiative (SCI) monitoring and evaluation activities funded through the Bill and Melinda Gates Foundation; PI: JPW, a European Commission 'Specific Research Project grant' CONTRAST (FP6 STREP contract no: 032203, http://www.eu-contrast.eu; PI: JPW), and a Wellcome Trust grant (no: 095778; PI: AE). Northern Tanzania sample collection was funded by the Schistosomiasis Consortium for Operational Research (SCORE) from the University of Georgia Research Foundation Inc., funded by the Bill & Melinda Gates Foundation (Sub-awards RR37–053/4787466 & RR374-053/4785426; PI: JPW). FA, AE, MR and the Schistosome Collection at the Natural History Museum (SCAN: AE) were supported by Wellcome grant 1045958/Z/13/Z (PI: AE). JAC, MB and JPW were supported by a European & Developing Countries Clinical Trials Partnership (EDCTP) grant FibroScHot (Ref RIA2017NIM-1842, PIs JAC, MB & JPW). JSM and SKP were supported by the National Institutes of Health (R01-AI145871, PI: JSM). SRD is supported by a UKRI Future Leaders Fellowship (MR/T020733/1). For the purpose of Open Access, the authors have applied a CC BY public copyright Licence to any Author Accepted Manuscript version arising from this submission.

Author contributions

DJB conceived and designed the study with input from JAC, MR, AE, FA, SB, MB, JSM and JPW. TC, NBK, EMT, PHLL and JPW planned and coordinated the collection of samples from Bugoto and Bukagabo Beach schools, which was carried out by TC, PHLL and MA. SCORE Tanzanian samples were collected by AG, BLW, FA, HN, JI, MR, RA, SK, and JPW in partnership with local technicians. CONTRAST samples were collected by CS, JRS, BW, and JPW in partnership with local technicians. JTV, RS and AE provided information on the Koome Island samples. MR, AE and FA curated the SCAN collection and coordinated sample delivery. HH coordinated the isolation and delivery of the two passaged Senegalese laboratory isolates, and NH performed DNA extraction and coordinated sequencing for those

samples. For all other samples, DJB extracted and amplified DNA, and planned and coordinated the sequencing. JSM and SKP performed Ca^{2+} reporter assays and modelling analysis. DJB analysed all other data and wrote the paper with input from JSM, SRD and JPW. S-KP, TC, JAC, MR, AE, BLW, PHL, SB and MB provided comments on the text, and all authors viewed and approved the final manuscript.

Competing interests: Authors declare that they have no competing interests.

Data and materials availability: The sequencing data generated in this study have been deposited in the European Nucleotide Archive (ENA) repository under project accession codes PRJEB42451 and PRJEB29904. Individual sample accessions are listed in Supplementary Data 14. The genome assembly and annotation files are available through ENA (PRJEA36577; GCA_000237925). The code used for data analysis is available at https://github.com/duncanberger/SM_VARIATION.

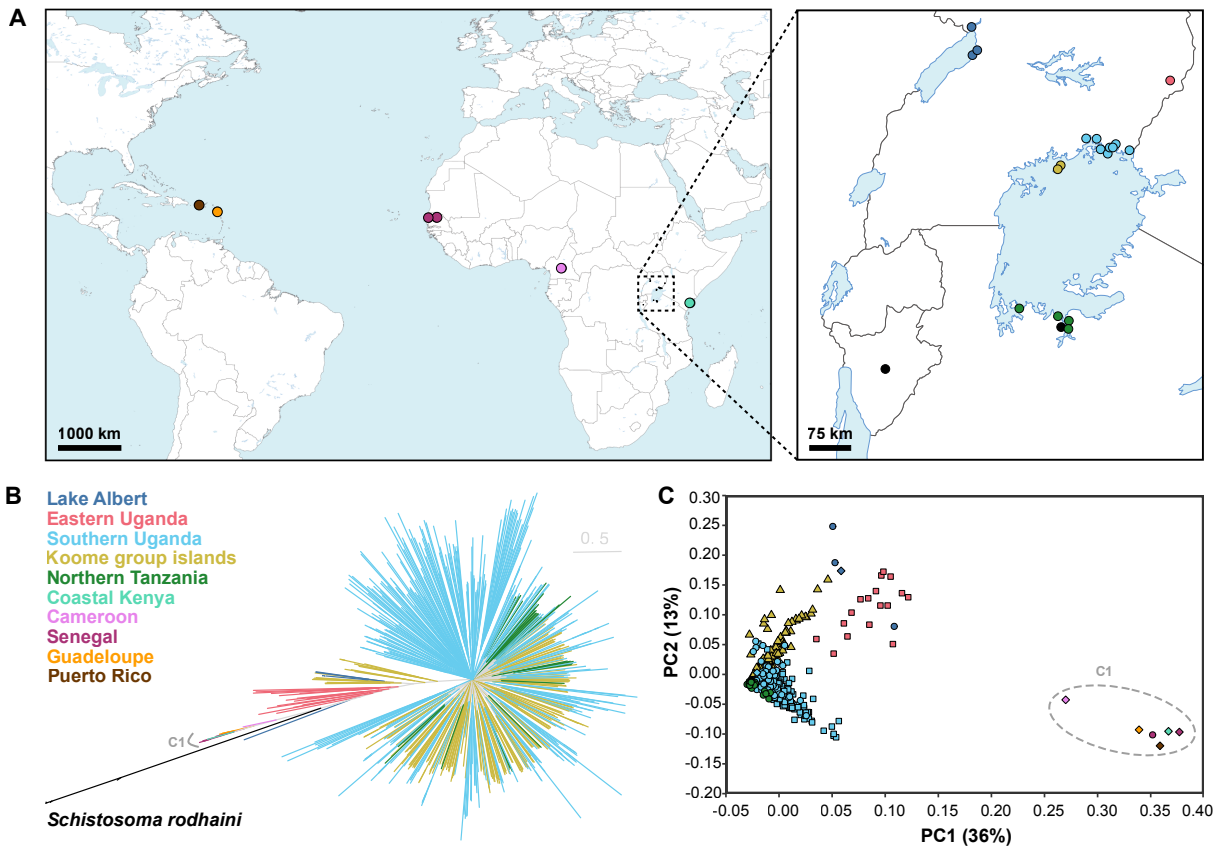
A
1000 km
75 km
B
Lake Albert
Eastern Uganda
Southern Uganda
Koome group islands
Northern Tanzania
Coastal Kenya
Cameroon
Senegal
Guadeloupe
Puerto Rico
0. 5
C1
Schistosoma rodhaini
C
PC2 (13%)
PC1 (36%)
C1
0.30
0.25
0.20
0.15
0.10
0.05
0.00
-0.05
-0.10
-0.15
-0.20
-0.05
0.00
0.05
0.10
0.15
0.20
0.25
0.30
0.35
0.40

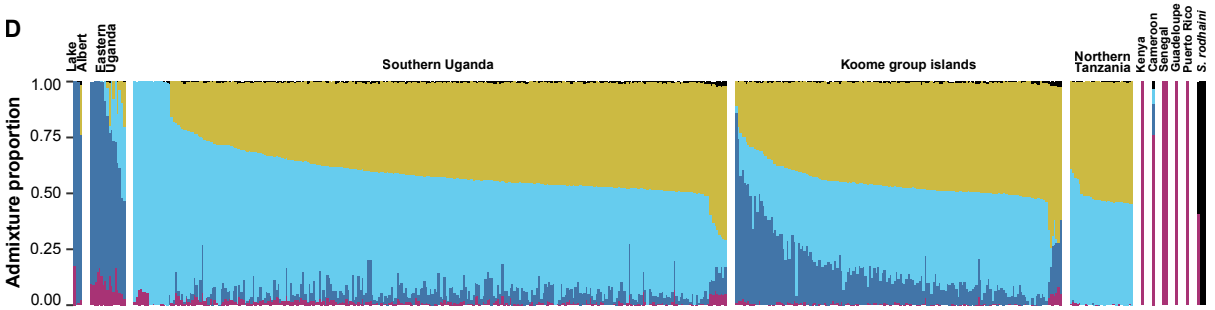
D
Lake Albert
Eastern Uganda
Southern Uganda
Koome group islands
Northern Tanzania
Kenya
Cameroon
Senegal
Guadeloupe
Puerto Rico
S. rodhaini
Admixture proportion
1.00
0.75
0.50
0.25
0.00

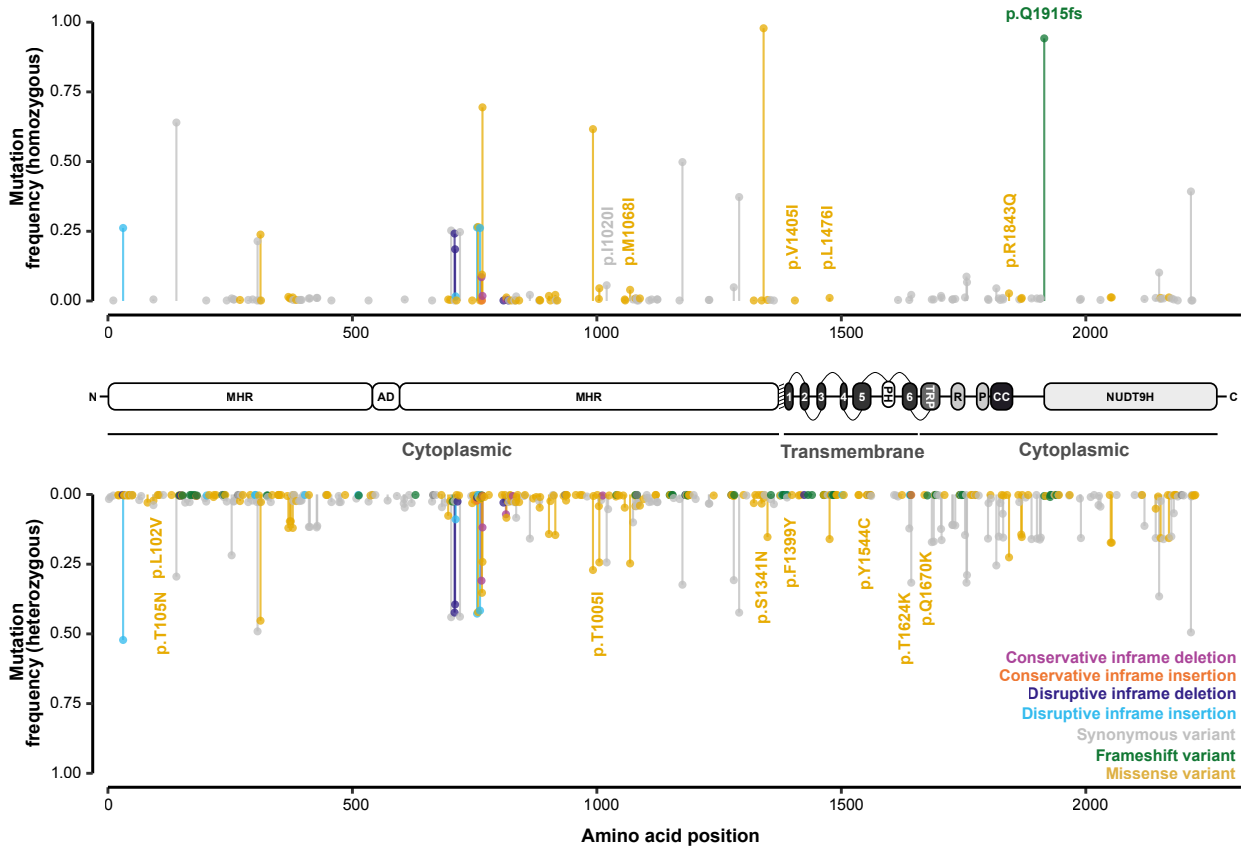
Mutation frequency (homozygous)
1.00
0.75
0.50
0.25
0.00
p.Q1915fs
p.I1020I
p.M1068I
p.V1405I
p.L1476I
p.R1843Q
0
500
1000
1500
2000
N
MHR
AD
MHR
1
2
3
4
5
HB
6
PDI
R
P
CC
NUDT9H
C
Cytoplasmic
Transmembrane
Cytoplasmic
Mutation frequency (heterozygous)
p.T105N
p.L102V
p.T1005I
p.S1341N
p.F1399Y
p.Y1544C
p.T1624K
p.Q1670K
Conservative inframe deletion
Conservative inframe insertion
Disruptive inframe deletion
Disruptive inframe insertion
Synonymous variant
Frameshift variant
Missense variant
Amino acid position

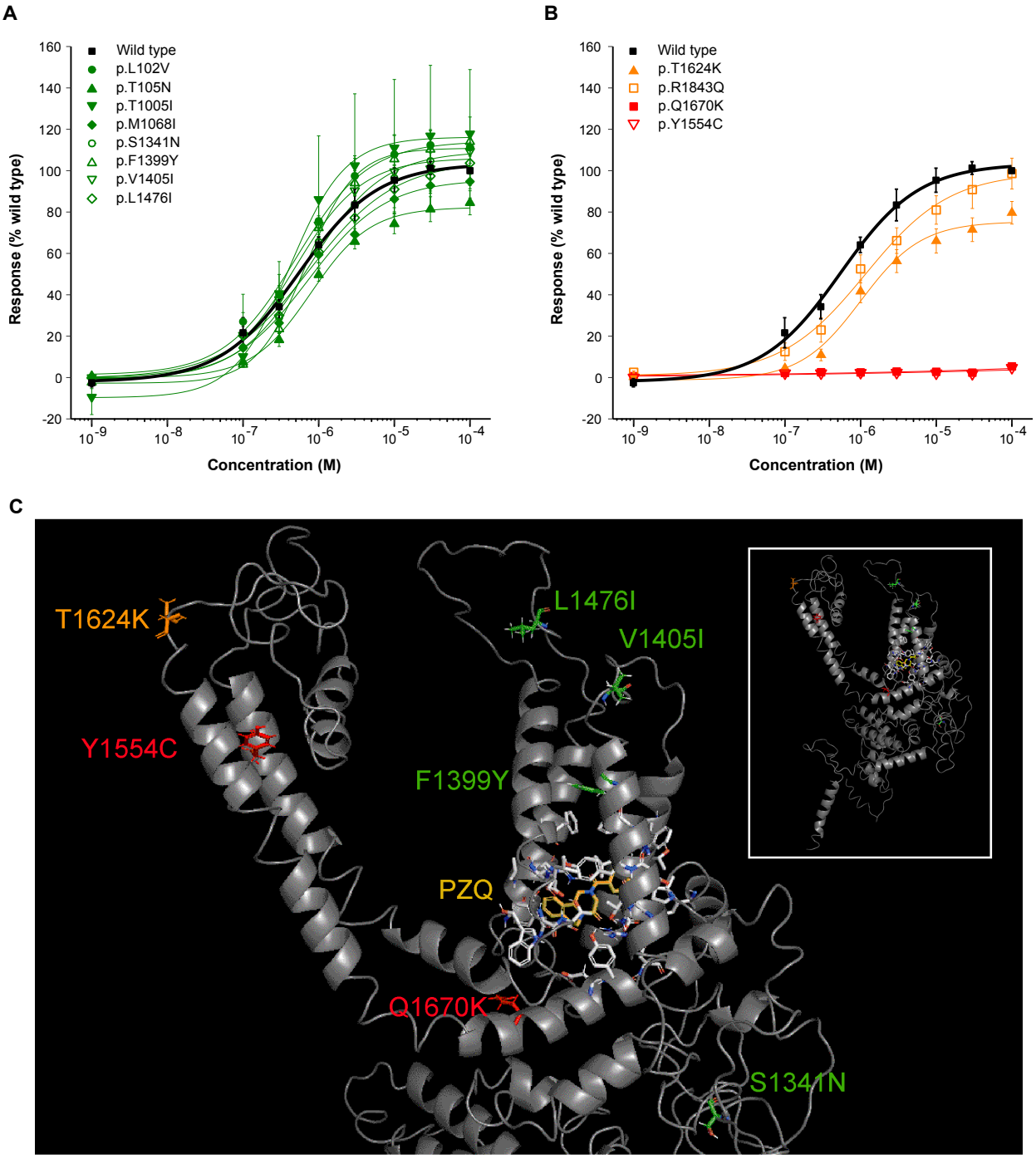
A
Wild type
p.L102V
p.T105N
p.T1005I
p.M1068I
p.S1341N
p.F1399Y
p.V1405I
p.L1476I
Response (% wild type)
Concentration (M)
B
Wild type
p.T1624K
p.R1843Q
p.Q1670K
p.Y1554C
Response (% wild type)
Concentration (M)
C
T1624K
Y1554C
L1476I
V1405I
F1399Y
PZQ
Q1670K
S1341N

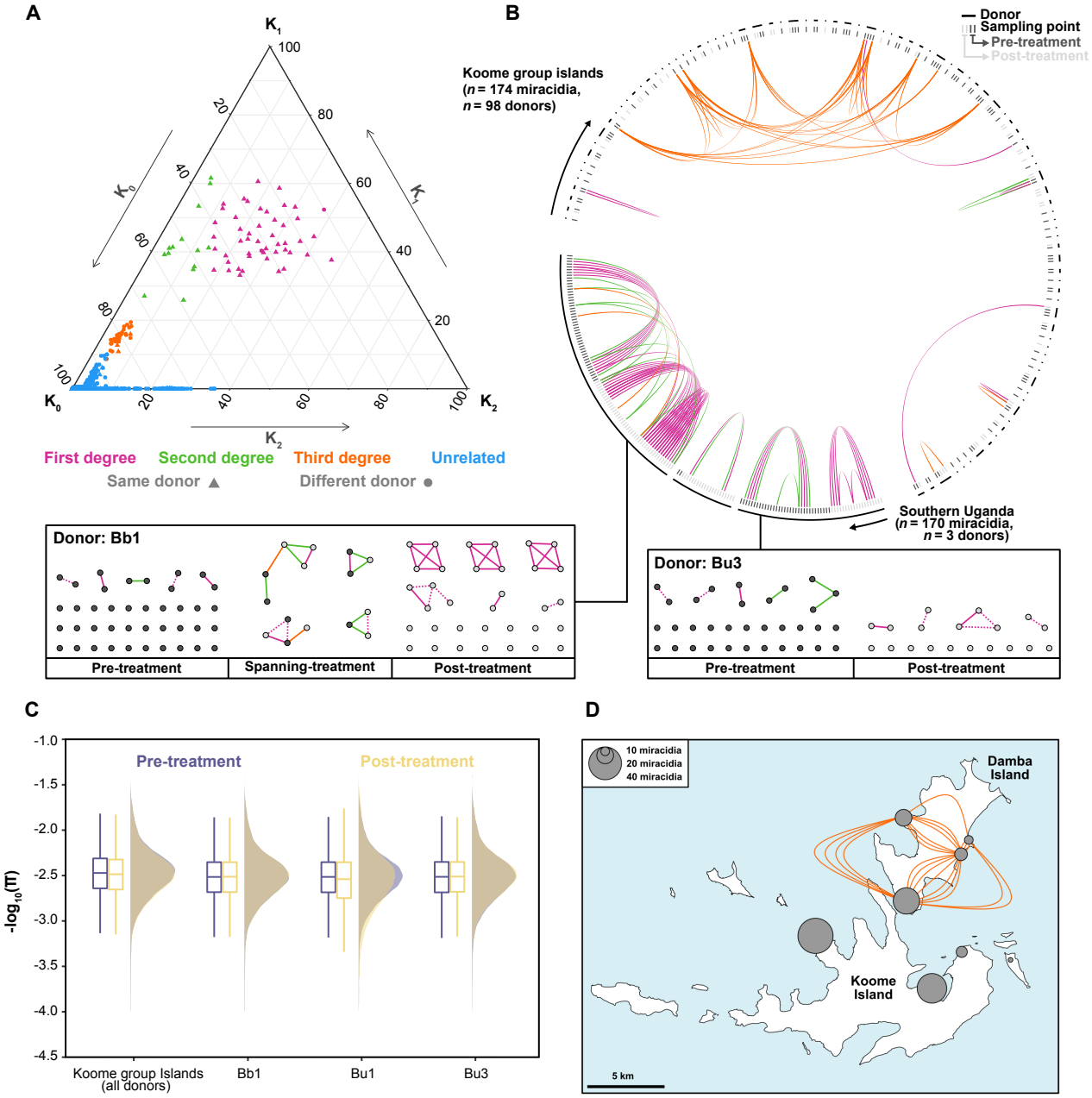
A
K1
K0
K2
First degree
Second degree
Third degree
Unrelated
Same donor
Different donor
B
Donor
Sampling point
Pre-treatment
Post-treatment
Koome group islands
(n = 174 miracidia,
n = 98 donors)
Southern Uganda
(n = 170 miracidia,
n = 3 donors)
Donor: Bb1
Pre-treatment
Spanning-treatment
Post-treatment
Donor: Bu3
Pre-treatment
Post-treatment
C
-log10(π)
Pre-treatment
Post-treatment
Koome group Islands
(all donors)
Bb1
Bu1
Bu3
D
10 miracidia
20 miracidia
40 miracidia
Damba
Island
Koome
Island
5 km